



EFFECT OF BLAST LOADING ON REINFORCED CONCRETE BUILDINGS

1CHANDRA SHEKHAR RAMAN, 2NEERAJ JAIN
1STUDENT, 2PROFESSOR
1RNTU BHOPAL,
2RNTU BHOPAL

ABSTRACT

Terrorists mainly target high occupancy residential and public buildings in order to claim maximum number of lives and cause extensive damage to the property. A bomb explosion within or immediately nearby a building can cause catastrophic damage on the building's external and internal structural frames, collapsing of walls, blowing out of large expanses of windows, and shutting down of critical life-safety systems. Loss of life and injuries to occupants can result from many causes, including direct blast-effects, structural collapse, debris impact, fire, and smoke. The indirect effects can combine to inhibit or prevent timely evacuation, thereby contributing to additional casualties. In addition, major catastrophes resulting from gas-chemical explosions results in large dynamic loads, greater than the original design loads, of many structures. Most of these structures have been or are built without consideration of their vulnerability to such extreme events. Therefore, the vulnerability assessment of buildings to explosion is important to provide mitigation strategies to protect the building's occupants and the property.

Due to the threat from such extreme loading conditions, efforts have been made during the past three decades to develop methods for analysis and design of structures to resist blast loading. Studies were conducted on the behavior of structural concrete subjected to blast loads and these studies gradually enhance the understanding of the role that structural details play a significant role in affecting the behavior. The response of various multi-storied reinforced concrete (RC) buildings subjected to constant axial loads and lateral blast loads was examined. For the response calculations a short duration, lateral blast load was applied and the response time history was calculated. The research mainly involved four important areas. These are blast load calculation by various codes, numerical modeling in SAP 2000, material characterization under high strain rates and non-linear dynamic structural analysis. The response and damage of various RC framed buildings for different blast load scenario were investigated.

The analysis and design of structures subjected to blast loads require a detailed understanding of blast phenomena and the dynamic response of various structural elements. Comprehensive and economical design strategies must be developed for future design considerations. Overall, this research broadens the current knowledge of blast response of RC framed structures and recommends methods to evaluate the blast mitigation strategies of multi-storey buildings.

CHAPTER - 1

INTRODUCTION

Chapter 1

INTRODUCTION

Explosives are mostly used in demolition of structure after their useful life. In recent times, there is significant increase in number of terrorist attacks around the world. Explosives have become common terrorist weapon as they are easy to produce, are compact and possess large power to cause serious damage on structures, injuries and death to civilians. Due to day-to-day advancement in military technology around the world, size of explosives is reduced and its devastating power is increased tremendously. Now a days, it is easy to carry and place explosives near public gathering places. Civilian buildings, government buildings and areas with large population density (i.e., stadium, railway stations, shopping centre, airports etc.) are becoming major bombing targets.

Some recent explosions are:-

Ronan Point (1968)

It was a block of flats in London. There were 22 storey's, with 5 flats per storey. This was constructed from prefabricated concrete elements.

There was an explosion in 18th floor in one of the flats. The explosion was a result of a gas leak. The explosion blew out one of the external load bearing walls from the structure. The removal of the load bearing wall resulted in the floors above 18th floor collapsing onto it. The impact of this collapse caused further failure of the floors below it. In this accident, four people were killed and 17 were injured. The end result of the explosion was partial collapse of the floors on one corner of the building. [Rasbash *et al.*(2004)]

WTC (1993)

On the day of February 26th 1993, a van containing a bomb was detonated into the second level basement car parking area underneath the world trade centre. It caused considerable to the basement level of structure. Despite the damage, the building was repaired and remained in use till 2001. On 2001 an aircraft strike into both WTC1 and WTC2 occurred, which resulted into complete collapse of the buildings. [Manning.(1993)] Similarly, the attack on the Twin Towers of the World Trade Centre in New York City, September 2001 was responsible for the death of 3000 people [Asaeda.(2007)]



Figure 1.1 (a)

Figure1.1 (b)

Figure 1-1: Bomb attack on Murrah Federal Building in Oklahoma City, 1995(a) before the (b) after the attack. [Osteraas.(2006)]

Oklahoma (1995)

The bombing of the Alfred P. Murrah Federal Building in Oklahoma City occurred on April 1995. It was the result of truck bomb which carried around 2,177 kg of fertilizer and fuel oil was detonated. The explosion destroyed 3 front columns of the Murrah Federal Office building which was a 9 storey reinforced concrete framed building. The destruction of 3 columns leads to progressive collapse mechanism. The level of destruction to the building was large. Around 167 people were killed and between 648 and 782 were injured. The building was ultimately

demolished within 2 months from the date of bombing. Figure 1.1 shows the picture of structure before and

after the attack [Craighead *et al.*(2009)]

Manchester (1996)

On 16th June 1996, in Manchester City Centre, a car bomb was detonated. The charge mass was 1500kg. The explosion caused considerable damage of property. However due to emergency response, no one was killed but over 200 persons were injured. The injuries were mainly due to broken glazing falling from buildings around the point of the explosion. A dozen buildings suffered structural damage. About one half of these had to be demolished. [Williams *et al.* (2000)]

Saudi Arabia (1996)

The Khobar towers bombing attack in was caused by a truck bomb of more than 9000kg TNT equivalent weight, placed near the fence 22m from the building. [Grant]

Reims (2013)

In Reims, France, an explosion caused by a gas leak partially destroyed a 5-storey block of flats, killing 3 people. [BBC news.(2013)]

Buenos Aires (2013)

On the 6th of August 2013, an explosion occurred which reduced 9 storey's of a 10 storey building to a pile of rubble. The cause of the explosion was believed to be a gas leak. [CBS news(2013)]

The threat of terrorist activities cannot be stopped but structural damage causing the loss of life can be minimized. These extreme events have created the need of a thorough study of the behavior of structure subjected to blast loads.

The term Blast means release of huge amount of energy from the source which lasts for very small fractions of time. Explosion produces vibration waves and causes vibration damages to the structure. When a small charge explodes, on external space of structure, pressure wave is generated which creates impulsive load on building. It propagates from source point approximately in spherical wave fronts, and after hitting, the wave front is reflected and modified. Figure 2.1 shows the Visual representation of building subjected to air blast showing the impact of positive and negative phases on the structure.

Mathematically the blast load is treated as triangular load. Application of blast loads is similar to wind loads but with different impulse which acts for short periods of time.

Explosive materials may be classified according to their physical state as solids, liquids or gases. Detonation of Explosives can produce severe over- pressure, primary and secondary fragments, fire, heat, ground shock etc.

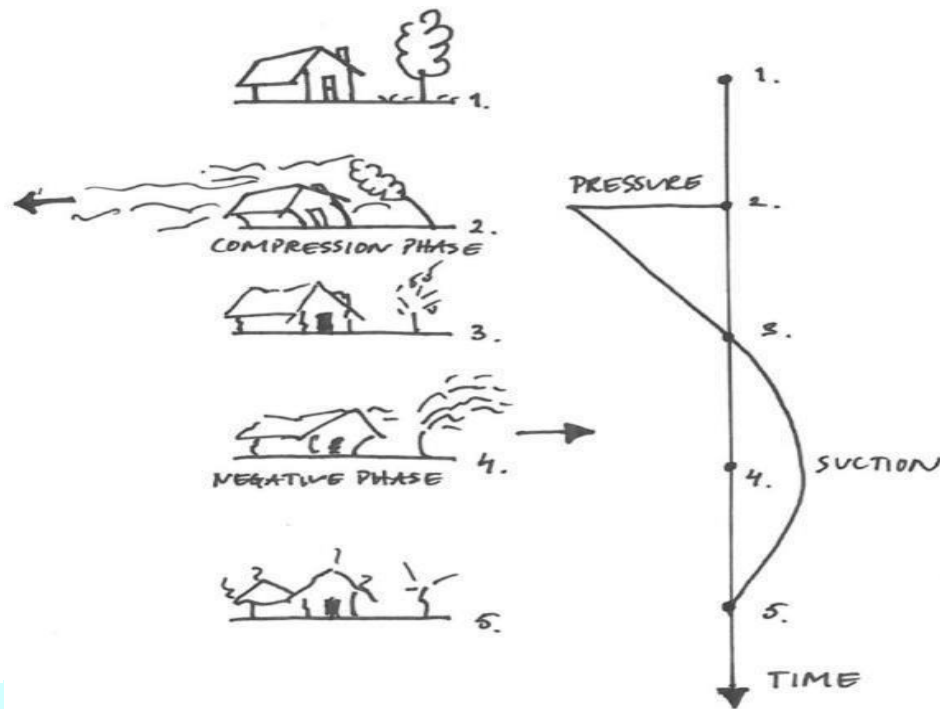


Figure 1.2: Schematic picture of building subjected to air blast. [Johansson (2002)].

The explosion can occur inside or outside the structure and causes damage to structural and non- structural elements of building, and also cause fatalities.

General buildings are not designed for blast loads. Time history function is used to express blast phenomena. Analysis of structure under blast load requires good knowledge of blast phenomena and dynamic response of structural elements. The blast load design aims to improving structural integrity of structure instead of complete collapse of structure.

It can be shown that with the present knowledge and software's, it is possible to perform analysis and evaluate their response.

CHAPTER - 2

LITERATURE REVIEW, OBJECTIVE AND SCOPE OF PRESENT WORK

Chapter 2

LITERATURE REVIEW, OBJECTIVE AND SCOPE OF PRESENT WORK



2.1 Literature review

Fu (2013) studied the strength of a tall structure under blast loading. He conducted finite element analysis on 3-D, 20 storey building by using the software ABAQUS to study its behavior under blasting. Detonation of bomb of charge weight 15 kg was simulated on the 12th floor of the structure. The effect of blast loading was considered through removal of certain columns without considering the duration of blast load. From this, it was concluded that, the 20 storey building designed using given design guidelines; these types of small scale bombs can hardly trigger the process of progressive collapse of building.

Elsanadedy *et al.* (2014) studied progressive collapse behavior of multi storey steel structure, due to blast. Model was analyzed using the finite element software LS-DYNA. Various blast scenarios were created by removing columns at various locations on ground floor. The results show that building may undergo progressive collapse for a charge weight of 500kg which can be easily carried by any small vehicle. They advised strengthening of outer ground floor columns by encasement of concrete or by steel plates. For the case where strengthening is not enough, it was suggested to have some structural modifications like diagonal bracing or shear walls.

Hrvoje draganic *et al.* (2012) In their paper, the work was carried out on calculation of blast load and its effect on structure. The blast load was analytically determined as a pressure-time history. The numerical model of structure was created in software SAP 2000. The analysis consists of estimation of risk, load according to estimated hazard and analysis of structural behavior. The analysis is carried out by sudden removal of column considering total destruction of column. The main aim of the work was to check demanded ductility of structure and to compare with available one. The deformation was also checked for the limits.

Patil *et al.* (2016) In their paper the response of 3 dimensional soft storey building with bare frame under blast loading is studied. Effect of variable blast source weight is calculated for 30m standoff distance. The blast load was analytically determined as pressure-time history and was applied on beam column joint of front face of building and numerical model was created in software SAP2000 for frame and soft storey building. The results show that due to infill there is significant reduction in displacement, velocity and acceleration. The

influence of blast load in terms of peak deflection, velocity and acceleration was determined and compared.

T. Ngo *et al.* (2007) Their paper titled “Blast loading and Blast Effects on Structures” gives an overview on the analysis and design of structures subjected to blast loads phenomenon to understand the blast loads and dynamic response of various structural elements subjected to blast loads.. This study helps for the design consideration against extreme cases like bomb blast, high velocity impacts etc.

Alexander M. Remennikov. (2003) studied the methods for predicting bomb blast effects on buildings. When a single building is subjected to blast loading produced by the detonation of high explosive device. Simplified analytical techniques used for obtaining conservative estimates of the blast effects on buildings. Numerical techniques including Lagrangian, Eulerian, Euler- FCT, ALE, and finite element modelling used for accurate prediction of blast loads on commercial and public buildings.

Silva *et al.* (2009) identified a procedure to estimate damage from some blast load scenarios by conducting a series of experiments for RC slabs. Other structural components such as load bearing key columns need a similar investigation to identify the blast response and damage of members.

Ronald L. Shope. (2006) studied the response of wide flange steel columns which were subjected to constant axial load and lateral load due to blast. The finite element program ABAQUS was used to model member by taking various slenderness ratio and boundary conditions. Blast loads were considered non-uniform. Changes in displacement time history value and plastic hinge formations resulting from varying the axial load were examined in the paper.

Goel *et al.* (2017) Their paper titled Collapse behavior of RCC building under blast load presents the investigation of critical columns of a four storey RCC building. Investigation is carried out by considering the load path where maximum behavior change occurs after removal of load bearing members in terms of displacement, vertical reaction and axial forces. It was observed that for load transfer and joint displacements, ground floor columns are most critical.

Khatavakar *et al.* (2016) In their paper, the importance of standoff distance is studied. Two high-rise structures (Closed Structure and Open RC frame Structure) were subjected to blast overpressure at distances

of 0.030 km, 0.050 km, 0.070 km, 0.090 km, 0.110 km and 0.150 km respectively. The minimum distance at which the structure is safe against the blast force was found for both the structural cases. A finite element tool, ETABS was used for the numerical analysis.

Ibrahim *et al.* (2017) In their paper finite element analysis was performed using software ABAQUS to analyze structural performance of RC frames under blast loading. A two dimensional 4-storey RC frame was modeled. The response of structure under blast load was presented along with two alternative designs. The results showed that by changing the design of external column, the response of structure was improved, especially by using concrete filled steel tube section.

Hashemi A and Mosalam K.M. (2004) In their Paper computational models subjected to blast loading were presented using the finite element method. Non linear transient analysis of reinforced concrete frames with and without unreinforced masonry infill wall was done. The models were used to investigate different parameters like loading duration and effect of masonry in filled wall on damage accumulation. Damage was globally quantified by maximum drift and maximum base shear in the RC frames. Local representation of damage in terms of reinforcing steel strains and yield was also discussed. Analysis results demonstrated that presence of the masonry infill walls significantly improves the overall behavior of structure for different loading durations.

Goel *et al.* (2012) presents various empirical relations available for calculation of blast load in the form of pressure-time function for the case of explosion in air. Various blast wave parameters are computed using equations. Various blast computation equations, charts, and references are provided in a concise form at a single place. Recommendations are also provided to choose suitable technique from available methods to compute the pressure-time function for obtaining response of structure.

Shallan *et al.* (2014) in their paper investigates the effects of blast loading on three buildings with different aspect ratios through numerical simulations. Finite element program AUTODYN was used to develop finite element model of structures. Blast loads were applied at two different locations and spaced from the building with different standoff distances. The results revealed that the effect of blast load decrease with increase in standoff distance from the building. With variation the aspect ratios of the buildings there is no variation in the displacement of the column. With increasing the aspect ratio the effect of blast load decreases in other element of the building.

Meghanadh M and Reshma T. (2017) Their paper presents effect of blast loads on a 5 storey R.C building . the charge weight was 100kg Tri nitro toluene (TNT). Point of detonation was 40m away from the building. Blast loads was calculated as per IS: 4991-1968. Force time history analysis was performed in software STAAD Pro. The influence of blast loads on structure was compared to that of same structure in static condition, The parameters like peak displacements, velocity, acceleration were studied.

Khan *et al.* (2017) investigates the effects of different structural configurations, member orientations and point of detonation on blast-induced failure of steel frame buildings through development of fragility curves. Three steel frame buildings were analyzed under blast load. The steel frame buildings were modeled and analyzed for dead load (DL), live load (LL) and seismic load (SL) for the National Capital Region (NCR), India. Force-controlled static nonlinear pushover analyses were performed to develop the fragility curves. Different orientations of the columns (I-section) were considered to investigate the effect on building fragility under the effect of blast load. The result shows significant effects of the structural configurations and column orientations on the blast resistance of the building. It was observed that the corner of a building is less critical in terms of mitigation of blast load.

Saatcioglu *et al.* (2011) analyzed the response of RC columns of a 10-story building under several blast scenarios. The columns were designed for seismic forces representative of Ottawa and Vancouver. A SDOF model was used to analyze the column. Consideration was given to the effect of column confinement. The force-deformation relationship for the concrete section was based on the curves derived from a moment-curvature analysis. Constant values for the dynamic and strength increase factors (DIF and SIF), were used in the analysis. The results showed that the columns with higher levels of seismic detailing performed better under the effect of blast load.

2.2 OBJECTIVE AND SCOPE OF THE PRESENT WORK

OBJECTIVE:

- To analyze and design the structures against the abnormal loading conditions like blast loads, detailed understanding of blast phenomenon is required.
- The main objective of the research presented in this thesis is to analytically and numerically study the structural behavior of RC Building subjected to blast loading by changing various charge weights and stand-off distances

- To study the effect of plastic hinge on structural response.

SCOPE OF THE STUDY:


To achieve the above-mentioned objectives the following tasks have been carried out:

- All the computation of dynamic loading on several RC building structures to evaluate the blast pressure.
- Computation of the blast loading on the structure.
- Modeling of several RC building in SAP 2000.
- Time history response of structure under the Blast loading.

CHAPTER - 3

OVERVIEW OF BLAST LOADING

Chapter 3



OVERVIEW OF BLAST LOADING

3.1 Explosion and blast phenomenon

Blast means sudden release of very large amount of energy from the source which lasts for very small fractions of time (in the range of few milliseconds to microseconds). Blast produces vibration waves and these waves cause damages to the structure. The detonation of a condensed high explosive generates hot gases with pressure up to 30×10^8 Pascal and a temperature of about 3000-4000⁰ C [Ngo *et al.* (2007)]. When a charge explodes on external space of building, pressure wave is generated that creates impulsive load on

building. The wave propagates from source point in approximately spherical wave fronts and upon hitting the wave front is reflected. As the blast wave expands its strength decays, velocity decreases and duration increases. Blast load is usually considered as linearly decaying triangular load for simplification. Application of blast loads is same as that of wind loads but with difference is that blasting is an impulsive action with a large amount of load having short duration. Explosions can be categorized on the basis of their nature as physical, nuclear and chemical events.

Physical explosion: Energy can be released from the failure of a cylinder of a compressed gas, volcanic eruption or mixing of two liquid at different temperature.

Nuclear explosion: Energy is released from the formation of different atomic nuclei by the redistribution of the protons and neutrons within the inner acting nuclei.

Chemical explosion: The rapid oxidation of the fuel elements (carbon and hydrogen atoms) is the main source of energy.

The magnitude and distribution of the blast loads on the structure arising from these pressures are function of the following factors:

1. Type and amount of explosives
2. Stand-off distance (location of detonation relative to structure)
3. Strength and geometry of structures.

3.2 Explosive types and weight

Explosives can be placed in various vehicles and depending upon that mass of explosives, estimated quantities of explosives in various vehicles is shown in Table 3.1. There are various types of explosives. They differ from each other in properties such as: rate of detonation, velocity, density, generation of heat. Trinitrotoluene (TNT) is generally used as the standard or reference explosive. Other explosives can be converted to as equivalent weight of TNT as shown in Table

3.2. The equivalent weight of an explosive is based on blast pressure.

of explosives in various vehicles [Chiranjeevi and Simon(2016)]

Vehicle types	Charge mass (kg)
Compact car truck	115
Trunk of a large car	230

Closed van	680
Closed truck	2270
Truck with a trailer	13610
Truck with two trailers	27220

3.3 Types of explosion

Blast load on structures can be divided into two main groups based on the confinement of the explosive such as confined and unconfined explosion.

3.3.1 Unconfined explosion

Unconfined explosion can be classified into three categories such as free air burst explosion, air burst explosion and surface burst explosion.

Table 3.2: Equivalent charge weight for 1 ton TNT [Chiranjeevi and Simon (2016)]

Explosives	TNT equivalent (kg)
TNT	1000
Compound B	1148
RDX	1185
HMX	1256
Nitroglycerin	1480
Gelatin	1000
Nitroglycerin dynamite	600
Semtex	1250
C4	1340

(a) Free air burst explosion

It is the explosion that occurs in free air. It produces an initial output whose shock wave propagates away from the center of the blast, and striking the structure without intermediate amplification of its wave from ground

as shown in Fig. 3.1 and usually it has spherical shape.

(b) Air burst explosion

The explosives which are located at such a distance from and above the structure that the ground reflections of the initial wave occur before the arrival of the blast wave to the structure. A front known as the Mach front is formed by the interaction of the incident wave and the reflected wave from ground surface. The reflected wave is the result of the enhancement of the incident wave by the ground surface as shown in Fig. 3.2. As the wave propagates, mach front height increases. The increase in height is called as path of triple point, formed by intersection of initial, reflected and mach wave.

(c) Surface burst explosion

When the detonation is located very near or on the ground, it is called surface burst explosion. In this type of explosion, the initial shock is amplified at the point of detonation due to the ground reflections. The reflected wave merges with incident wave at the point of detonation to form a single wave. It is similar in nature to mach stem, but its shape is hemispherical as shown in Fig. 3.3.

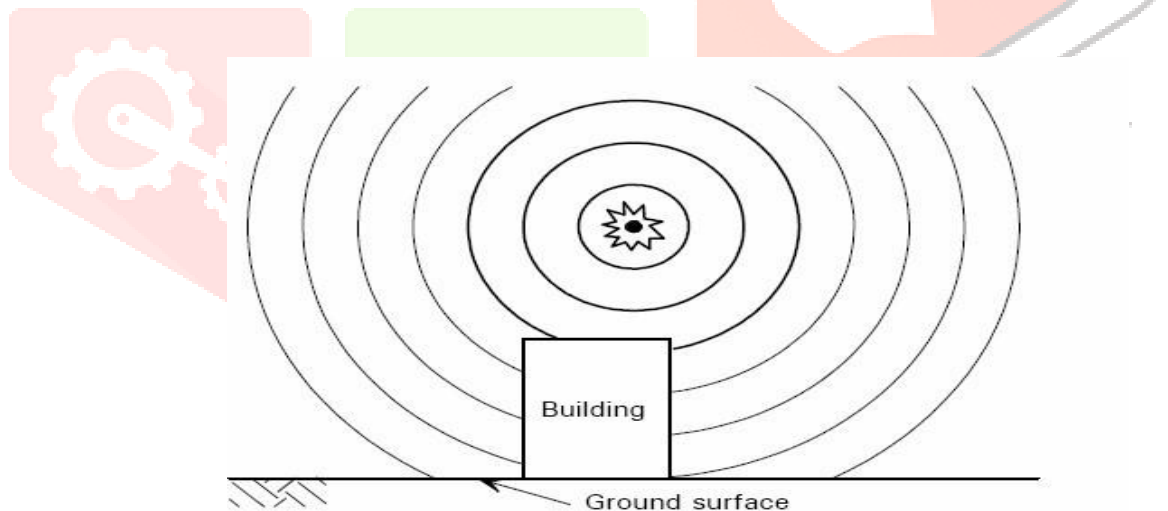


Figure 3.1: Free air burst explosion [Unified Facilities Criteria (2008)]

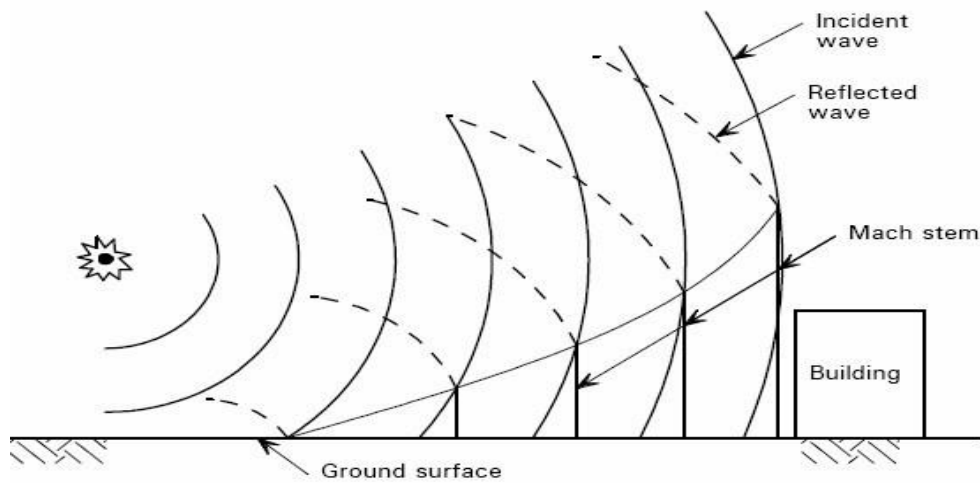


Figure 3.2: Air burst explosion [Unified Facilities Criteria (2008)]

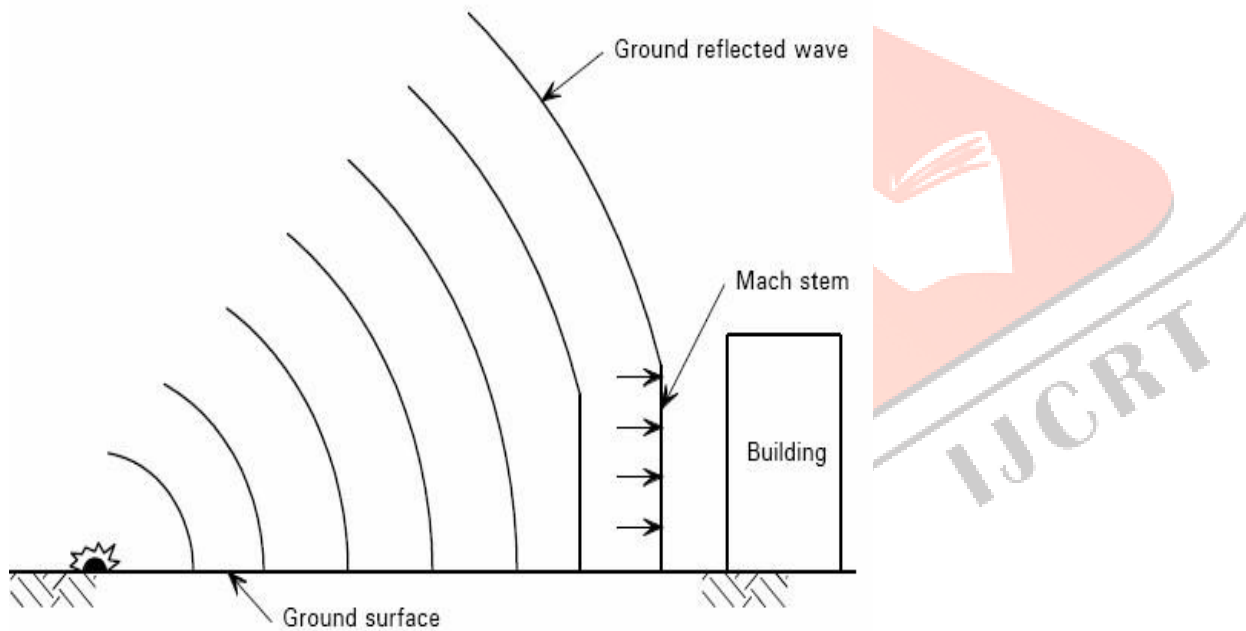


Figure 3.3: Surface burst explosion [Unified Facilities Criteria (2008)]

3.3.2 Confined explosions

Confined explosion can be classified into three categories such as fully vented, partially vented and fully confined explosion.

(a) Fully vented explosion

This type of explosion happens when the explosives are placed within or immediately adjacent to a barrier or cubicle type structure with one or more surfaces open to the atmosphere. The initial wave, amplified by the non-frangible portions of the structure and the products of detonation are totally vented to the atmosphere forming a shock wave which propagates away from the structure. Schematic of this type of explosion is shown in Fig. 3.4 (a).

(b) Partially Confined Explosion

Partially confined explosion can be referred to that type when the explosion occurs within a barrier or cubicle type structure with limited size openings. The initial wave, which is amplified by both frangible and non frangible portion of the structure, and the products of detonation are vented to the atmosphere after some finite period of time as shown in Fig. 3.4 (b).

(c) Fully confined explosions

Fully confined explosion is associated with either total or near total containment of the explosion by a cubicle structure as shown in Fig. 3.4 (c). Internal blast loads will consist of unvented shock loads and very long duration gas pressures. This type of explosion is the function of the degree of containment.

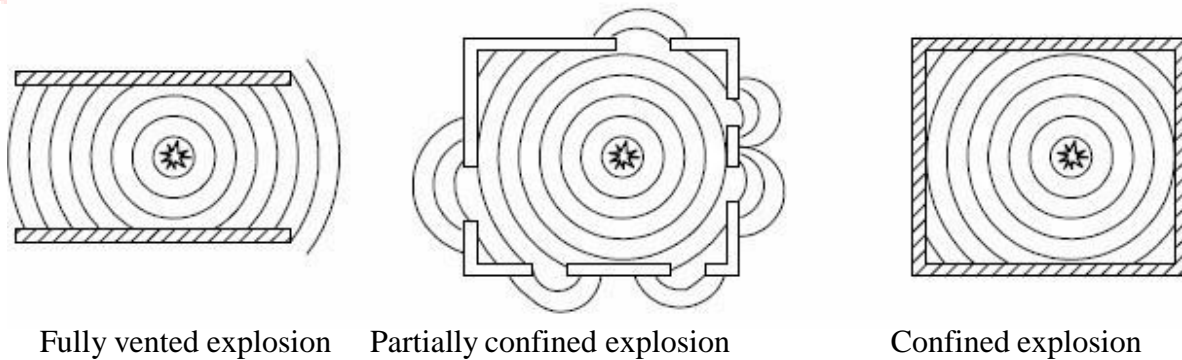


Figure 3.4: Confined explosions

3.4 Blast wave phenomena

For the case of a free air blast wave, Fig. 3.5 shows the idealized profile of the pressure with respect to time.

The wave reaches a point at a certain distance from the detonation. Initially the pressure surrounding the element is equal to the ambient pressure P_0 . When the shock front reaches that point it undergoes an instantaneous increase to a peak pressure P_{so} at the time of arrival t_A . The time needed for the pressure to reach its peak value is very small. For design purposes it is assumed to be equal to zero. This peak pressure P_{so} is also known as side-on overpressure or peak overpressure. The value of the peak overpressure as well as the shock wave velocity decreases with increasing distance from the detonation point. After the pressure reaches to its peak, it decreases with an exponential rate until it reaches the ambient pressure at time $t_A + t_0$, being called the positive phase duration. After the positive phase, the pressure becomes smaller (referred to as negative phase) than the ambient value, and finally returns to ambient pressure value.

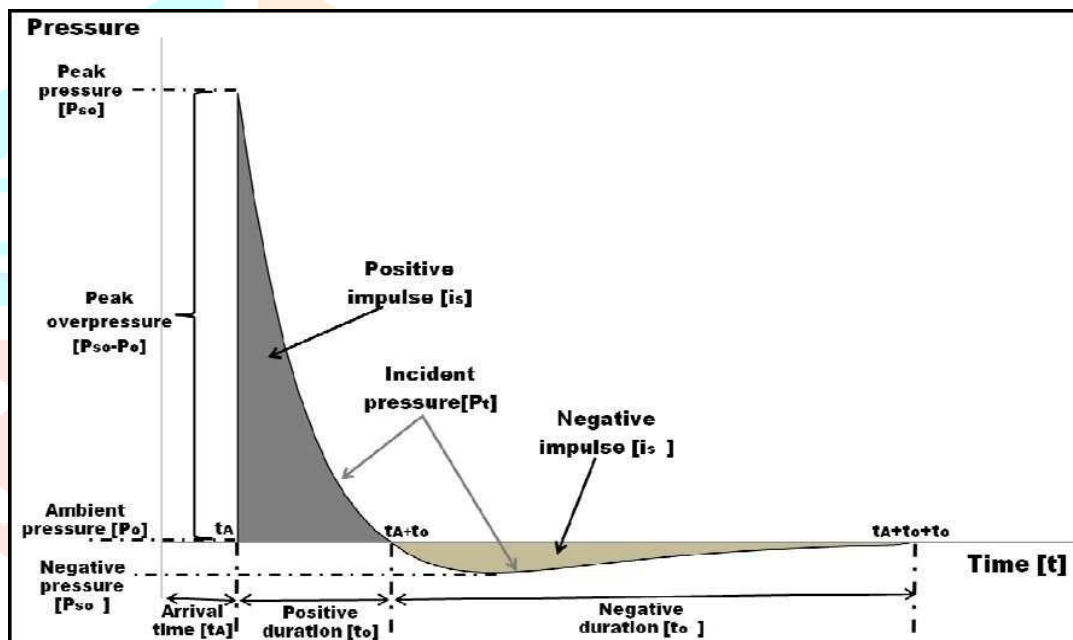


Figure 3.5: Pressure time history of blast wave [Karlos and Solomos (2013)]

The negative phase is longer than the positive phase and its minimum pressure value is denoted as P^- and its duration as t^- . In this phase the structures are subjected to suction forces. The negative phase of the wave is usually not taken into account for design purposes as the main structural damage is connected to the positive phase of blast pressure history. The pressures produced from the negative phase are relatively small compared to those of the positive phase.

3.5 Scaling law

One of the most critical parameters for blast loading is calculating the distance of detonation point from the structure of interest. The peak pressure value and blast wave velocity decreases rapidly by increasing the stand-off distance. Most common blast scaling laws are the ones introduced by Hopkinson-Cranz and Sachs. These laws have the ability to scale parameters, in order to be used for varying values of distance and charge weights. The idea behind this law is that during the detonation of two charges of the same explosive material that have similar

geometry but having different weights and are situated at the same distance from a target surface, similar blast waves are produced at the point of interest when the two explosives are under the same atmospheric conditions.

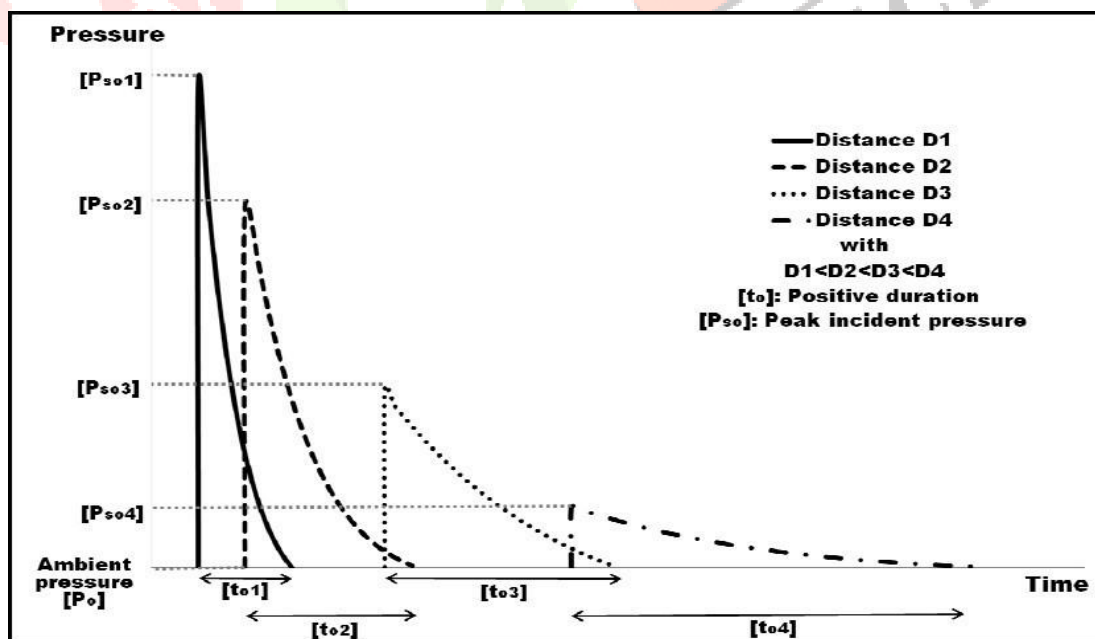
$$\text{Scaled distance} = \frac{R}{W^{1/3}}$$

(3.1)

here, R is the distance from the detonation source to the point of interest (m) and W is the weight of the explosive (kg).

W^3

on the blast positive pressure phase. [Karlös and Solomos(2013)]



3.6 Prediction of blast pressure

Estimations of peak overpressure due to spherical blast based on scaled distance $Z = R/W^{1/3}$ were introduced by Brode (1955) as:

$$P_{so} = \begin{cases} 1.13 \frac{P_{so}}{Z^3} & \text{for } P_{so} > 10 \text{ bar} \\ 0.975 \frac{P_{so}}{Z} & \text{for } P_{so} < 10 \text{ bar} \end{cases} \quad (3.2)$$

$$P_{so} = 6.7 + \frac{1.455}{Z^2} + \frac{5.85}{Z^3} - 0.019 \text{ bar} \quad (0.1 \text{ bar} < P_{so}) \quad (3.3)$$

Newmark and Hansen (1961) introduced a relationship to calculate the maximum blast overpressure, P_{so} , in bars, for a high explosive charge detonates at the ground surface as:

$$P_{so} = \frac{W^{1/3}}{R^3 + 93} \quad (3.4)$$

Another expression of the peak overpressure in kPa is introduced by Mills (1987), in which W is expressed as the equivalent charge weight in kilograms of TNT, and Z is the scaled distance

$$P_{so} = \frac{1772}{Z^3} - \frac{114}{Z^2} + \frac{108}{Z} \quad (3.5)$$

3.7 STRUCTURAL RESPONSE TO BLAST LOADING

Dynamic response of structure subjected to blast loading involves non-linear material behavior, high strain rate effects, the uncertainty in calculation of blast load and their duration and time dependent deformations. There are various methods to determine the response of a structure for transient loads. This includes multi-degree-of-freedom (MDOF), single-degree-of-freedom (SDOF) and approximate methods such as energy methods and static analysis methods (Yandzio *et al.* 1999).

To simplify analysis, some assumptions related to loads and response of structure has been given and is widely accepted. The structure can be idealized as single degree of freedom system (SDOF). The relation between positive phase duration and natural period of structure is established. It leads to blast load

idealization and simplifies the classification of blast loading conditions.

3.7.1 Elastic single degree of freedom system:

The main difference between structures under static and dynamic loading is the presence of inertia in the equation of motion. It is related to the mass of the system and, hence, the mass becomes an important consideration in dynamic analysis. Structures can in many cases be reduced to equivalent dynamic system having a similar behavior as the real structure. A typical Single degree of freedom system is the mass spring-damper system. It is shown in figure .Here the mass can move in a vertical direction only. In this system, the spring and damper are considered to having mass less. It is also assumed that the spring is linear. The force of gravity is omitted because the displacement of the mass y is measured from its neutral position, which the mass assumes the static case where no loading is applied.

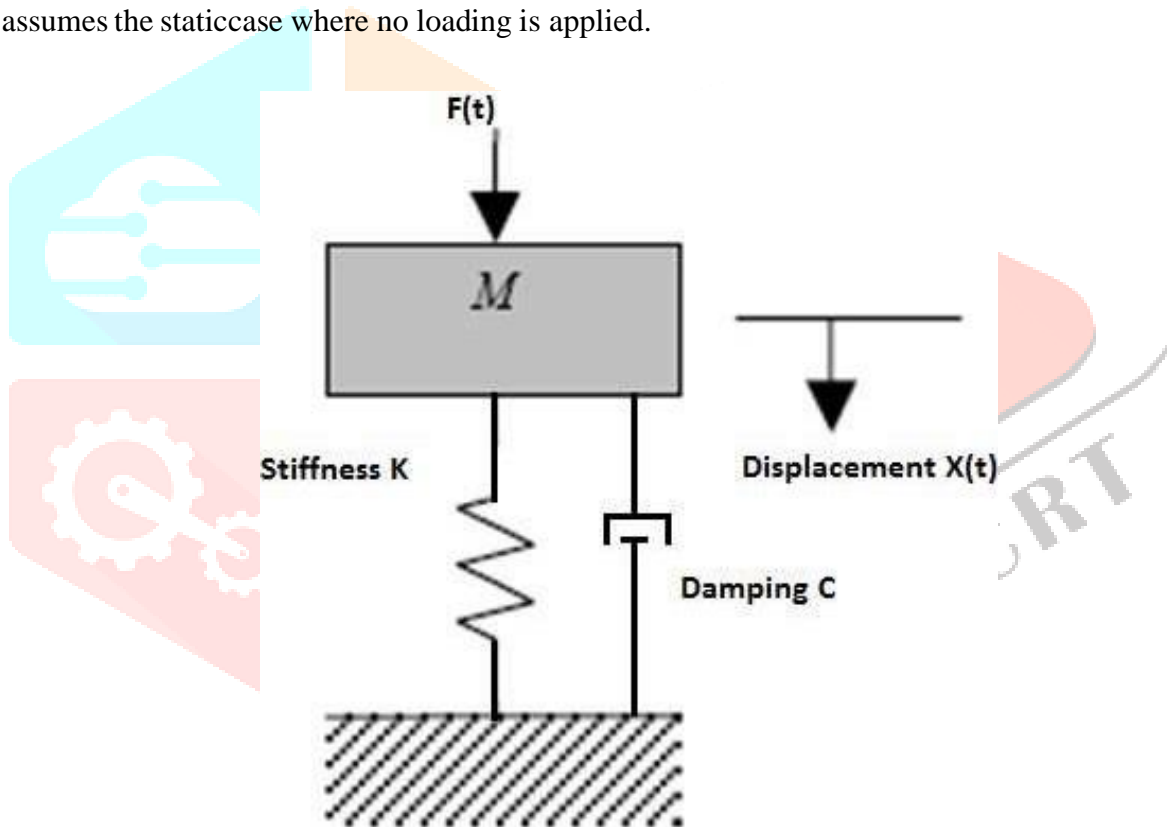


Figure 3.7: Single degree of freedom system

The equation of motion of the SDOF damped system subjected to an applied force $F(t)$ is

$$Mx'' + Cx' + Kx = F(t) \quad (3.6)$$

Here m is system mass, c is damping coefficient and k being system stiffness. The velocity is denoted by \dot{x} and \ddot{x} for the acceleration. The response of structural dynamic systems involves certain degree of damping. However, for the structures subjected to blast loads the effects of damping are not considered in the analysis as damping has very little effect on the maximum deflection, (Baker *et al.*, 1983). The reason is that structural damping is much lower than for other systems where critical damping needs to be considered.

Plastic response may be modeled with the use of SDOF analysis. Figure shows the idealized SDOF structure. Figure shows idealized blast wave.

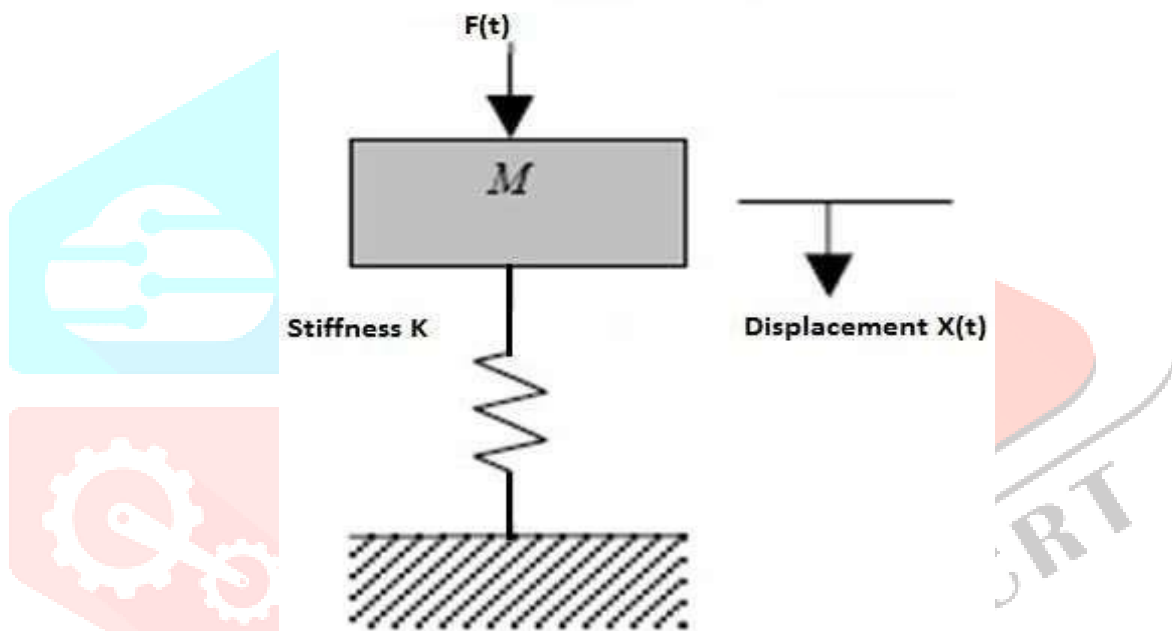


Figure 3.8: SDOF idealized structure (Ngo *et al.* 2007)

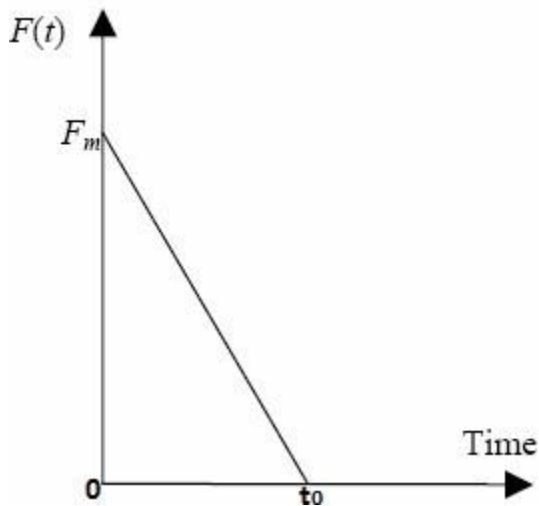


Figure 3.9: Idealized blast wave (Ngo *et al.* 2007)

The blast load can be idealized as a triangular pulse having a peak force F_m and Positive phase duration t_0 . The forcing function is given by

$$F(t) = F(m) \left(1 - \frac{t}{t_0}\right) \quad (3.7)$$

The impulse created by blast can be found by calculating area under the force-time curve, and is given by

$$\frac{I}{2} = \int_0^{t_0} F(t) dt \quad (3.8)$$

The equation of motion of the un-damped elastic SDOF system for a time ranging from zero to the positive phase duration t_0 , is given by Biggs (1964) as

$$Mx'' + Kx = F(m) \left(1 - \frac{t}{t_0}\right) \quad (3.9)$$

$$x(t) = \frac{F(m)}{K} (1 - \cos \omega t) + \frac{F(m)}{K t_0} \left[\frac{\sin \omega t - t}{\omega} \right] \quad (3.10)$$

$$x'(t) = \frac{F(m)}{K} [\omega \sin \omega t + 1 (\cos \omega t - 1)] \quad (3.11)$$

Here ω is the natural vibration frequency of the structure,



$$\ddot{\omega} = \frac{K}{M} \quad (3.12)$$

If maximum displacement, x_{max} occurs at time t_m , then the velocity becomes zero at the time of maximum displacement,

$$0 = [\omega \sin(\omega t_m) + \dot{\omega} (\cos(\omega t_m) - \cos(\omega t_0))] \quad (3.13)$$

This implies that

$$\omega t_m = f(\omega t_0) \quad (3.14)$$

Therefore, structural behavior under blast loads is influenced by ωt_0 and the loading regimes are classified as (Ngo et al. 2007)

- $\omega t_0 < 0.4$; impulsive loading regime
- $\omega t_0 > 40$; quasi-static loading regime
- $0.4 < \omega t_0 < 40$; dynamic loading regime

3.7.2 Elasto-Plastic SDOF Systems:

Structural elements undergo large inelastic deformation under blast loading. Exact dynamic response analysis is possible by step-by-step numerical solution, which requires nonlinear dynamic finite-element software. However, the degree of uncertainty in determination of the loading and interpretation of acceptability of the resulting deformation is such that solution of a postulated equivalent ideal elasto-plastic SDOF system (Biggs 1964) is mostly used. The

Interpretation is based on required ductility factor $\mu = \frac{\gamma_m}{\gamma_e}$ which is shown in figure

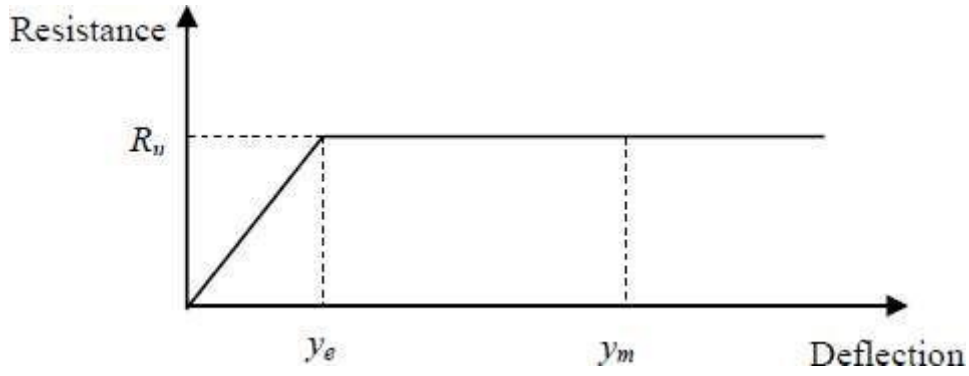


Figure 3.10: Simplified resistance function of an elasto-plastic SDOF system (Biggs 1964)



CHAPTER - 4



BEHAVIOUR OF MATERIALS AT HIGH STRAIN RATE

Chapter 4

BEHAVIOUR OF MATERIALS AT HIGH STRAIN RATE

4. Behaviour of materials at high strain rate

Blast loads produces very high strain rates in the range of $10^2 - 10^4 \text{ s}^{-1}$. The high loading rate alters the dynamic mechanical properties of target structures and also the expected damage mechanisms for various structural elements. Since the mechanical properties of plain concrete and steel are strain rate dependent, the behavior of structural members under extreme loading conditions can only be accurately predicted by considering the strain rate dependent properties of materials. For reinforced concrete structures subjected to blast loading, the strength of concrete and steel reinforcing bars can increase significantly due to high strain rate. Figure 4.1 shows the approximate ranges of the strain rates for different loading conditions. The normal static strain rate is located in the range: 10^{-6} - 10^{-5} s^{-1} , while blast pressures yield loads associated with strain rates in the range: 10^2 - 10^4 s^{-1} .

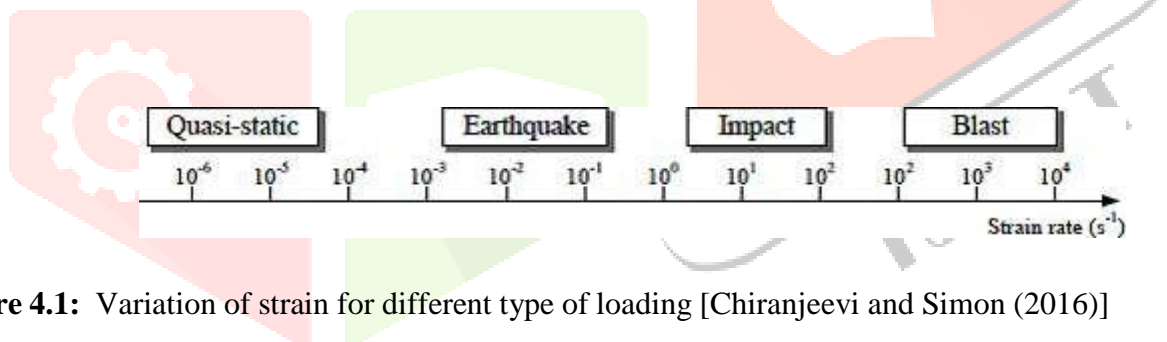


Figure 4.1: Variation of strain for different type of loading [Chiranjeevi and Simon (2016)]

4.1 Dynamic properties of concrete under high strain rates.

The mechanical properties of concrete under dynamic loading conditions can be different from that under static loading. While the dynamic stiffness does not vary a great deal from the static stiffness, the stresses that are sustained for a fixed period of time under dynamic conditions may gain values that are remarkably higher than the static compressive strength of material. Strength magnification factors as high as 4 in compression and up to 6 in tension for strain rates in the

range of 10^2 – 10^3 sec^{-1} have been reported (Grote *et al.* 2001) The DIF is often used to characterize the rate sensitive behavior of material and the strain rate effect on compression and tension of concrete is typically reported as the DIF (i.e. ratio of dynamic strength to static strength). Figure

4.2 shows the variation of stress-strain relationship with strain rate for grade 40 concrete (Ngo *et al.* 2007).

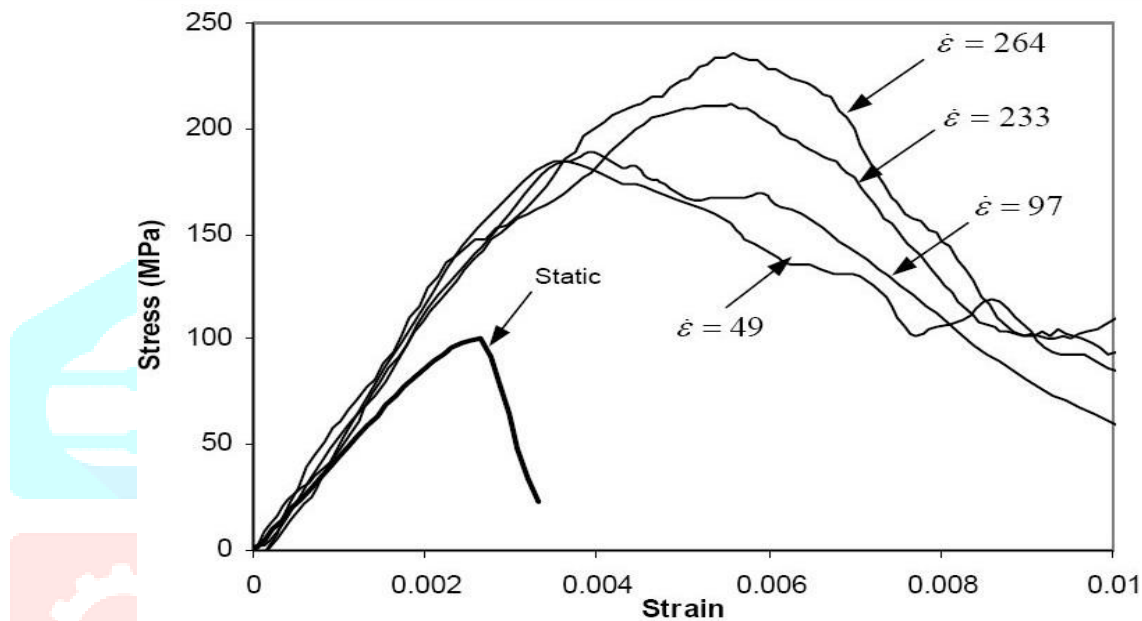


Figure 4.2: Stress-strain curves of Grade 40 MPa concrete at different strain rates (Ngo *et al.* 2007)

4.1.1 Compression.

CEB model code 1990 (CEB, 1993), the DIF for compressive strength of concrete is

$$\text{DIF} = \left(\frac{\varepsilon'}{\varepsilon'_s} \right)^{1.026\alpha_s} \quad \text{for } \varepsilon' \leq 30 \text{ s}^{-1} \quad (4.1)$$

$$\text{DIF} = \gamma_s \left(\frac{\varepsilon'}{\varepsilon'_s} \right)^{-1} \quad \text{for } \varepsilon' > 30 \text{ s}^{-1} \quad (4.2)$$

Here, ε' is strain rate in the range of $30 \times 10^{-6} \text{ s}^{-1}$ to 300 s^{-1} , $\varepsilon'_s = 30 \times 10^{-6} \text{ s}^{-1}$ is static strain rate and $\log \gamma_s = 6.156\alpha_s - 2$, $\alpha_s = 1/(5+9 f_{cs}/f_{co})$, where $f_{co} = 10 \text{ MPa}$ and f_{cs} is the static compressive strength Tedesco and Ross (1998) conducted a series of Split Hopkinson's Pressure Bar (SHPB) tests to investigate the effect of strain rate and moisture content on concrete strength. The DIF

equations for compression suggested by Tedesco and Ross (1998) are



$$DIF = 0.00965 \log_{10} \dot{\epsilon}' + 1.058 \geq 1.0 \quad \text{for } \dot{\epsilon}' \leq 63.1 \text{ s}^{-1} \tag{4.3}$$

$$DIF = 0.758 \log_{10} \dot{\epsilon}' - 0.289 \leq 2.5 \quad \text{for } \dot{\epsilon}' > 63.1 \text{ s}^{-1} \tag{4.4}$$

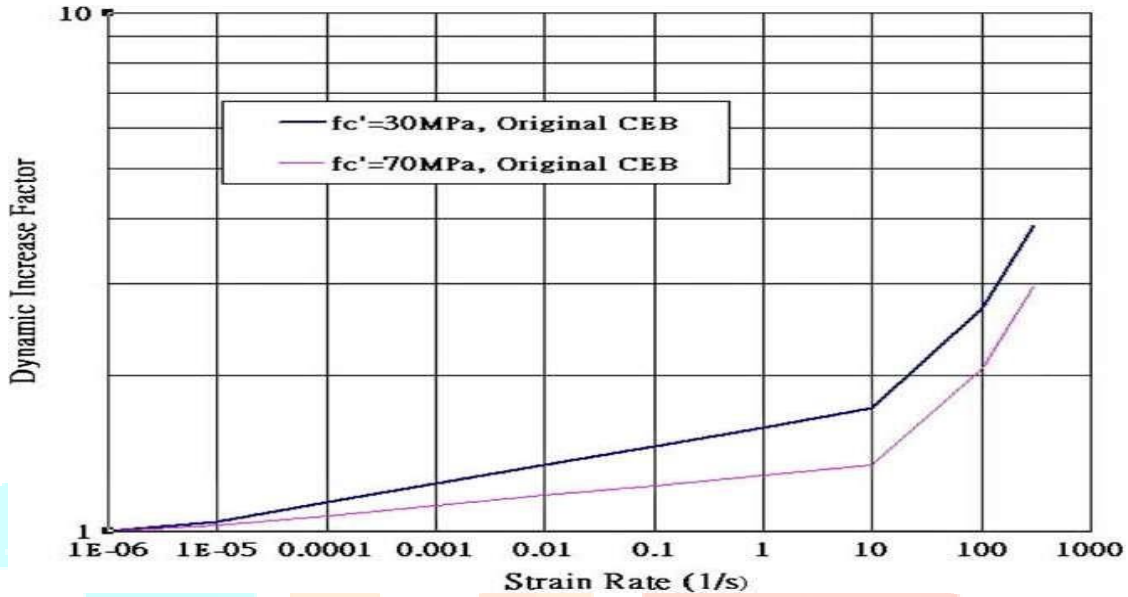


Figure 4.3: DIF variation over strain rate for concrete in compression (Bao *et al.* 2010)

Figures 4.3 show the DIF variation over the strain rate for concrete in compression (Bao *et al.* 2010).

4.1.2 Tension

Tedesco *et al.* (1997) conducted a series of dynamic tensile tests and, based on the results, proposed the following equations.

$$DIF = 0.1425 \log_{10} \dot{\epsilon}' + 1.833 \geq 2.32 \text{ s}^{-1} \quad \text{for } \dot{\epsilon}' \leq 2.32 \text{ s}^{-1} \tag{4.5}$$

$$DIF = 2.929 \log_{10} \dot{\epsilon}' + 0.814 \leq 6 \quad \text{for } \dot{\epsilon}' > 2.32 \text{ s}^{-1} \tag{4.6}$$

The DIF for tension as per CEB model code 1990 (CEB, 1993) is

$$DIF = \left(\begin{matrix} 1.016 \delta_s \\ \epsilon \end{matrix} \right) \quad \text{for } \dot{\epsilon}' \leq 30 \text{ s}^{-1} \tag{4.7}$$

ε's



$$\text{DIF} = \beta_s \begin{cases} 1/3 \\ \left(\frac{\dot{\epsilon}}{\dot{\epsilon}'_s}\right) \end{cases} \quad \text{for } \dot{\epsilon}' > 30 \dot{\epsilon}'_s \quad (4.8)$$

where $\dot{\epsilon}'$ is strain rate of range $3 \times 10^{-6} \text{ s}^{-1}$ to 300 s^{-1} . $\log \beta_s = 7.11 \delta - 2.33$, in which

$\delta_s = 1 / (10 + 6 f_{cs} / f_{co})$ where $f_{co} = 10 \text{ MPa}$ and f_{cs} is the static compressive strength of concrete. Figures 4.4 show

the DIF variation over the strain rate for concrete in tension, (Bao *et al.* 2010).

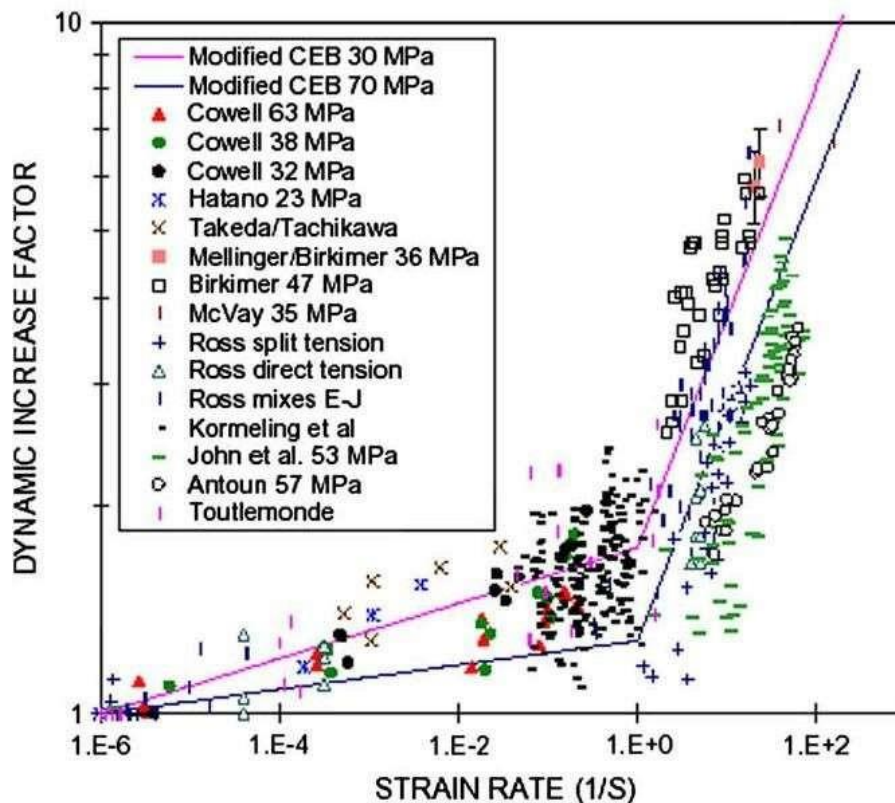


Figure 4.4: DIF variation over strain rate for concrete in tension (Bao *et al.* 2010)

4.2 Dynamic properties of reinforcing steel under high strain rates

Due to isotropic properties of metallic materials, their elastic and inelastic response to dynamic loading can easily be monitored and examined. Soroushian and Choi (1987), it was concluded that yield strength of steel is more sensitive to rate of strain than the ultimate strength. Young's modulus is independent of rate of straining. They said that the most important factor is static yield strength. The mechanical properties of steel of lower yield strength are more sensitive to rate of straining than higher yield strength steel.

Malvar (1998) studied strength enhancement of steel reinforcing bars under high strain rates. It was reported that the DIF of yield and ultimate stress is inversely related to the yield stress itself. It was described in terms of the dynamic increase factor (DIF), which can be evaluated for different steel grades and for yield stresses, ranging from 290 to 710 MPa and strain rates between 10^{-4} s^{-1}

and 10 s^{-1} . It is given by

$$DIF = \frac{1}{1 - \alpha \left(\frac{\dot{\epsilon}}{10^4} \right)^{0.5}} \tag{4.9}$$

Here, for yield stress calculation $\alpha = \alpha_{fy}$

$$\alpha_{fy} = 0.074 - 0.04(fy/414)$$

For ultimate stress calculation $\alpha = \alpha_{fu}$

$$\alpha_{fu} = 0.019 - 0.009(fy/414)$$

Where, $\dot{\epsilon}$ is the strain rate in s^{-1} and fy is the static yield strength of the reinforcement in MPa. Figure 4.6 shows the Stress-strain curves for steel for different strain rates. (Liew 2008)

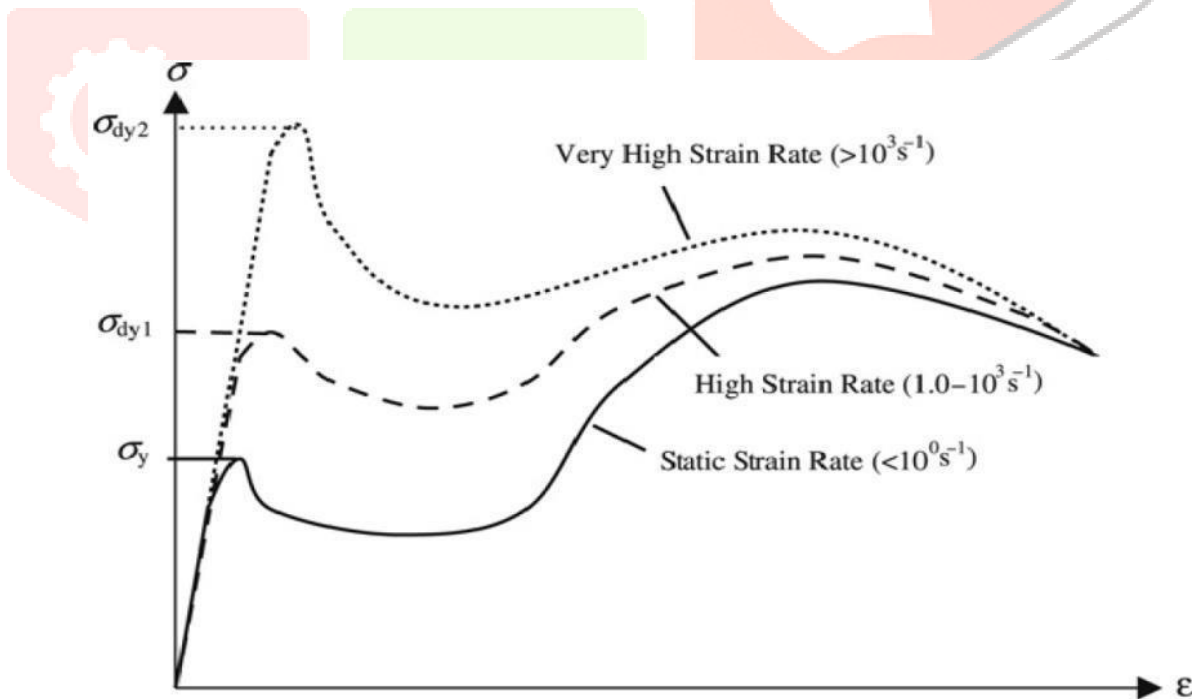


Figure 4.5: Stress-strain curves for steel for different strain rates (Liew 2008)

CHAPTER - 5



ANALYTICAL MODEL

Chapter 5

ANALYTICAL MODEL

In this study, 3-D reinforced concrete (RC) buildings were modeled in SAP 2000. Various buildings were modeled for various stand-off distances. Figure 5.1 shows the plan of 30 storey RC building.

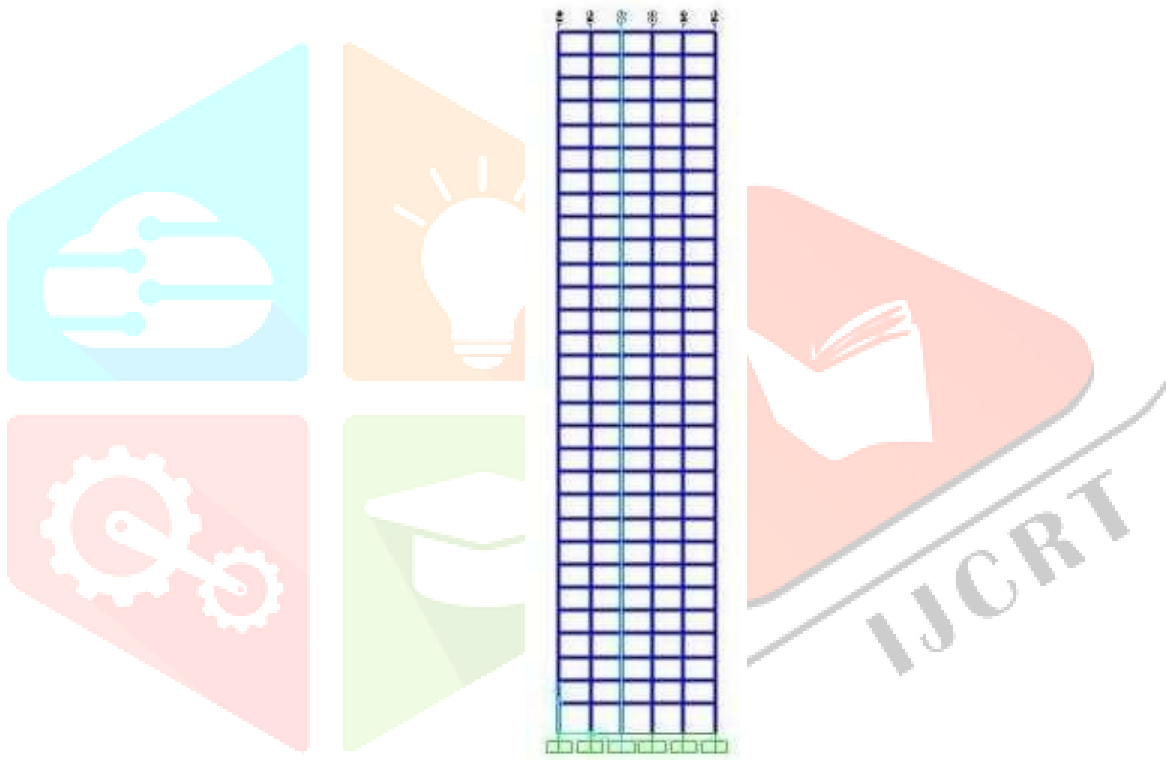


Figure 5.1: Elevation of 30 storey RC building.



Figure 5.2: 30 storey RC building model.

Figure 5.2 shows 3D model of 30 storey RC building. The charge weight used for the analysis was 1000 kg TNT. Stand-off distance, which is point of detonation, is 10 m and 5 m is used for the analysis. For stand-off distance of 10 m, two buildings each of 30 storey, 25 storey, 20 storey, 15 storey, 10 storey and 5 storey were modeled. All buildings have 5×5 bays in each direction where each longitudinal and transverse bay span is 4 m in length. Plan of the buildings are symmetrical. Height of building is 3 m at each floor except ground floor whose height is 4 m. Considered size of beam is 250×350 mm and size of column is 400×400 mm. Thickness of slabs is 120 mm. Beams and columns are modeled as frame element and slab is modeled as shell element. The building is designed as per Indian codes for dead and live load conditions. Concrete grade is assumed to be M30 and grade of reinforcement is Fe500. Strength of concrete and reinforcing bars was increased by a factor of 1.25 [IS: 4991 (1968)] due to the development of high strain rate under blast loading conditions.

For the first case, building with respectively 30, 25, 20, 15, 10 and 5 storeys were subjected to the blast loads. Material non linearity was incorporated in the analysis. Time history load were applied at each joint on the front face of the buildings.

In the second case, six other building with respectively 30, 25, 20, 15, 10 and 5 storeys were also modeled. Same input were applied for these building as that of the first case. Same load and time values were also applied on these buildings. The difference in the two cases is that in the second case hinges were also provided on each of the beams and columns of these six buildings. The hinge properties for beam elements were taken from tables in ASCE 41-13 as concrete beams–flexure. The non-linear hinges were of M3 type. The locations of hinges were 200 mm and 3800 mm respectively on the beams.

Hinge property for columns was also taken from tables in ASCE 41-13. The hinges were of P- M2-M3 type. They were designed for flexure/shear failure condition. The locations of hinges were 200 and 3800 mm for the columns on first floor and 150 mm and 2850 mm respectively on the column of other floors. The output values like displacement of joints, velocity acceleration, and base shear values were compared for both the cases.

Six other buildings of storey number respectively were also modeled. The storey numbers of these buildings were respectively thirty, twenty-five, twenty, fifteen, ten and five. All properties used were same like the first case. Same non-linear hinges were also provided on beams and columns. The value of blast load was considered as 1000 kg TNT. The stand-off distance was 5 m. The results were compared with the response of structures having stand-off distance of 10 m. The corresponding scaled distances are 0.5 and 1 m/kg^{1/3}.

Table 5.1: Major wave front parameters, their notations, scaling factor and units

Wave front parameter	Notation	Scaling factor	Units
Normally reflected pressure	P_r	1	<i>kpa</i>
Incident pressure	p_s	1	<i>kpa</i>
Normally reflected specific impulse	I_r	$1/W^{1/3}$	<i>Kpa.ms/kg^{1/3}</i>
Incident specific impulse	I_s	$1/W^{1/3}$	<i>Kpa.ms/kg^{1/3}</i>
Time of arrival	t_a	$1/W^{1/3}$	<i>ms/kg^{1/3}</i>
Positive phase duration	t_0	$1/W^{1/3}$	<i>ms/kg^{1/3}</i>
Wave front velocity	U	1	<i>m/ms</i>

The blast load was calculated as per the Canadian code [CSA Standard S850-12 (2012)]

$$x = C_0 + C_1 z + C_2 z^2 + C_3 z^3 + C_4 z^4 \quad (5.1)$$

$x = \ln(X)z = \ln(Z)$ Here,

x = a scaled wave front parameter as specified in table 5.1

Table 5.1 shows parameters, their notations, scaling factor and units Z = the scaled distance

Table 5.2: Coefficients of the fitting polynomials obtained for the wave front parameters of spherical TNT surface burst.

Wave front parameter	C_0	C_1	C_2	C_3	C_4
ly reflected pressure $0.06 < Z \leq 1.95$	8.9973	-2.6077	-0.5045	-0.0588	0
lly reflected pressure $1.95 < Z < 39.67$	9.7457	-4.7276	1.1734	-0.1337	0

Table 5.3: Coefficients of the fitting polynomials obtained for the wave front parameters of spherical TNT surface burst.

Wave front parameter	C_0	C_1	C_2	C_3	C_4
Positive phase duration $0.06 < Z \leq 0.5$	0.2966	3.7346	2.4367	0.481	0
Positive phase duration $0.5 < Z \leq 0.95$	0.5684	3.7267	0.9479	-0.8821	0
Positive phase duration $0.95 < Z \leq 1.55$	0.5400	2.5376	8.0273	7.8467	0
Positive phase duration $1.55 < Z \leq 3.2$	1.5967	-3.1675	3.2709	-0.7764	0
Positive phase duration $3.2 < Z < 39.67$	0.3458	0.849	-0.1814	0.0191	0

Table 5.2 and 5.3 provides the value of coefficients that are used to calculate blast overpressure and positive duration of blast wave respectively for different values of Z from equation 5.1.

In the third cases two 10 storey buildings were modeled in SAP. The joint load and time values were calculated as per [IS: 4991 (1968)] and Canadian code [CSA Standard S850-12 (2012)] respectively. The time history loads were applied on front face of the structure. The results were plotted and analyzed.

A modal analysis of 30 storey building was also conducted.

Blast load was applied on front face of building. The detonation point is considered along centerline of buildings. Figure 5.4 shows the position of detonation point from the building.

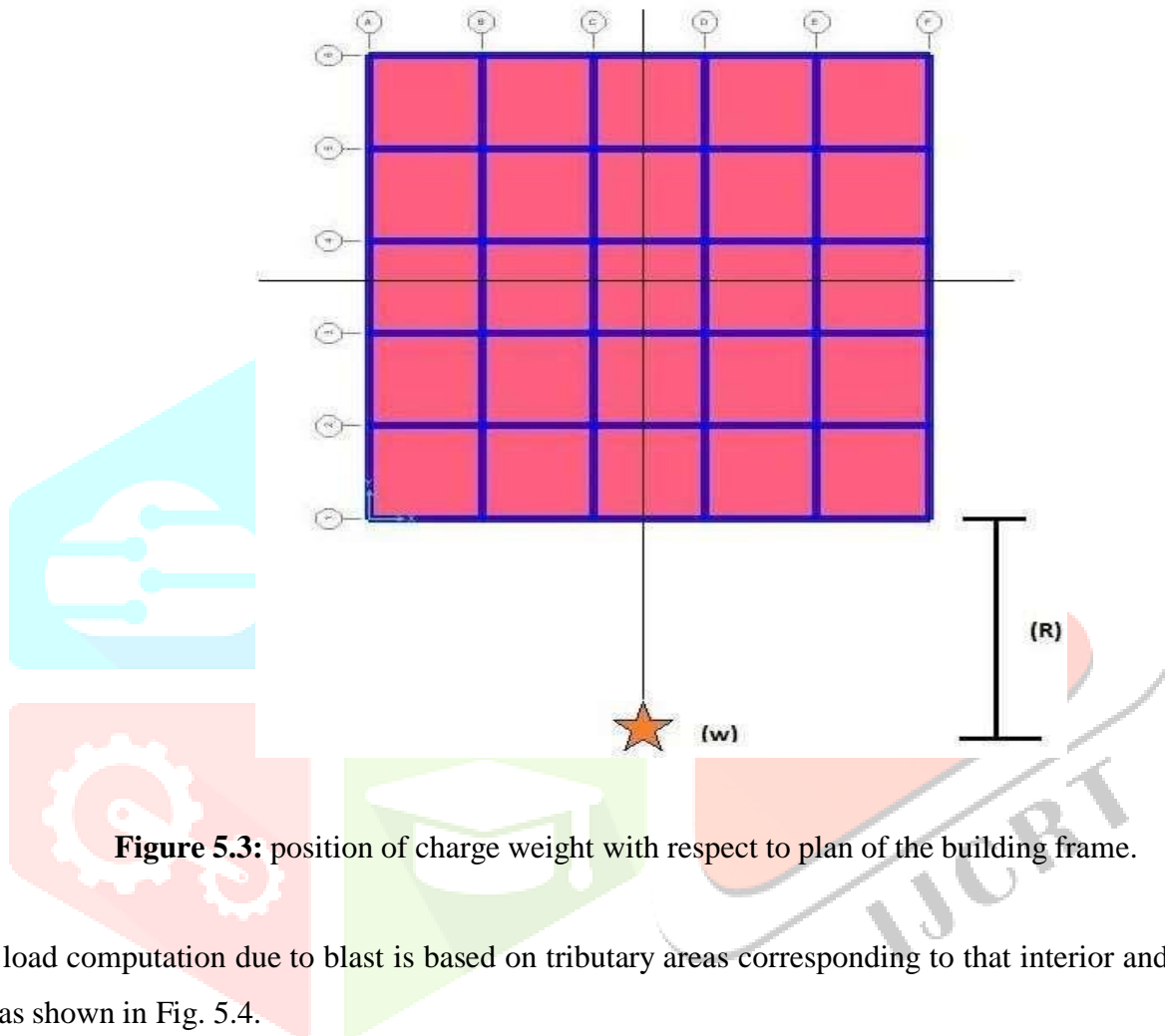
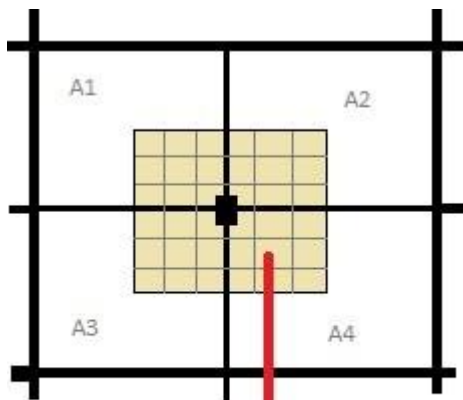
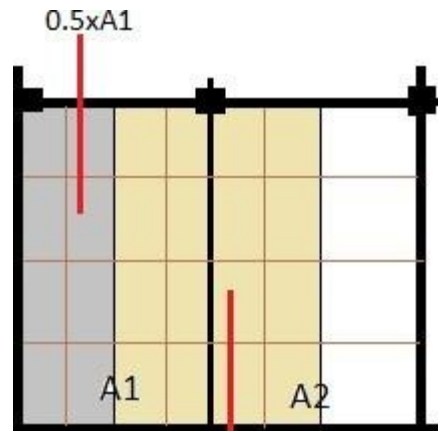


Figure 5.3: position of charge weight with respect to plan of the building frame.

Joint load computation due to blast is based on tributary areas corresponding to that interior and exterior joint as shown in Fig. 5.4.



$$0.25 \times (A1 + A2 + A3 + A4)$$



$$0.5 \times (A1 + A2)$$

Figure 5.4 (a): Tributary wall areas (interior joint).

Figure 5.4 (b): Tributary wall areas (corner/side joints).

Figure 5.4: Tributary wall areas for calculation of joint loads due to blast pressure.

CHAPTER - 6



RESULTS AND DISCUSSIONS

Chapter 6

RESULT AND DISCUSSIONS

6.1 Modal analysis

The analysis consists of finding the structural behavior of RC building subjected to blast loading. A modal analysis was conducted on 30 storey RC building. Natural time period and frequency of the structure was found by modal analysis of structure. Figure 6.1 shows the mode shape of first six modes of the structure.

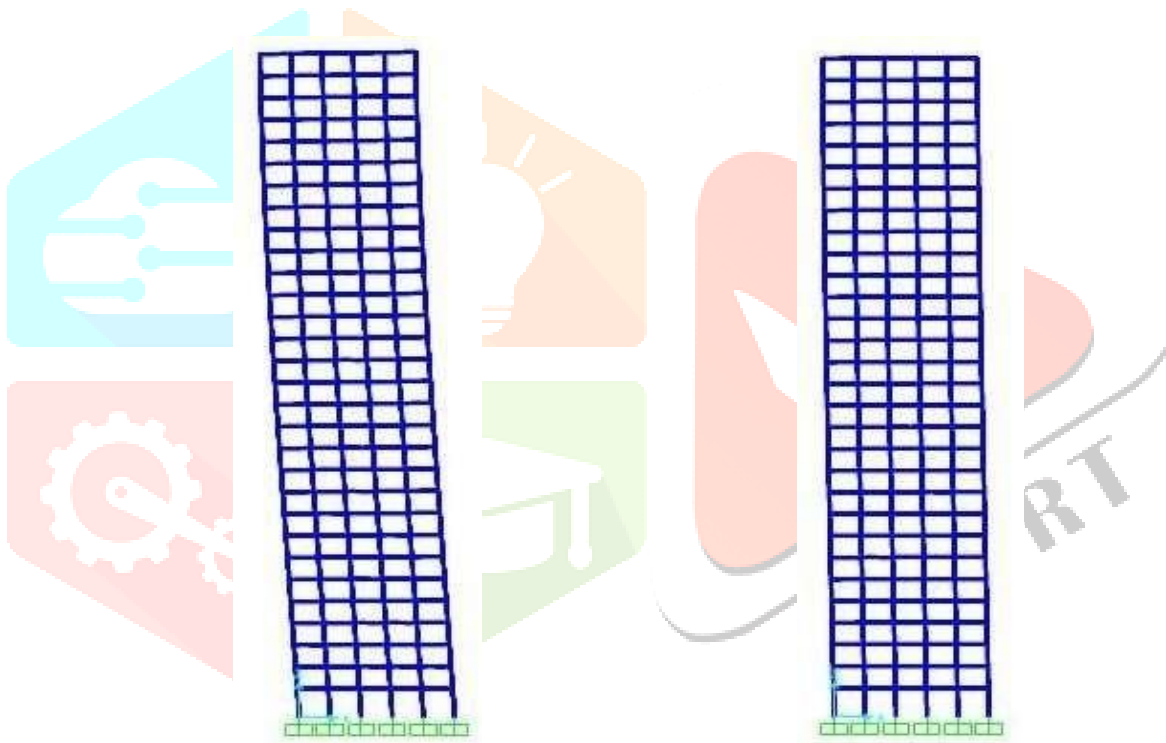


Figure 6.1 (a): Mode 1

Figure 6.1 (b): Mode 2

Figure 6.1: Mode shapes of the structure (continued)

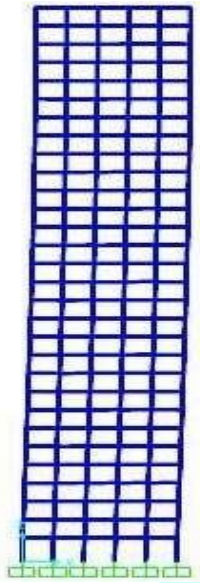


Figure 6.1 (c): Mode 3

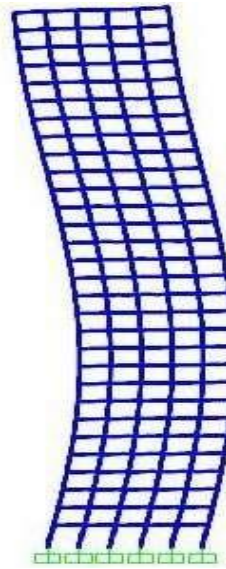


Figure 6.1 (d): Mode 4

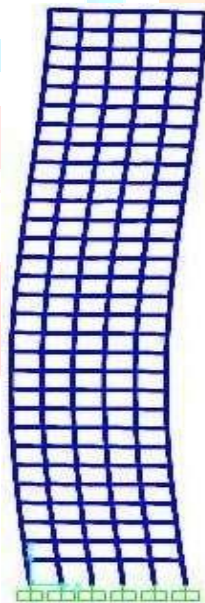


Figure 6.1 (e): Mode 5

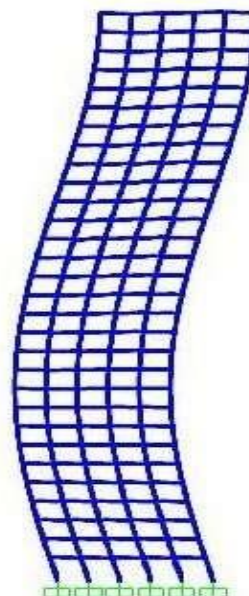


Figure 6.1 (f): Mode 6

Figure 6.1: Mode shapes of the structure

Table 6.1 shows typical time period and frequencies of 12 modes of structure.

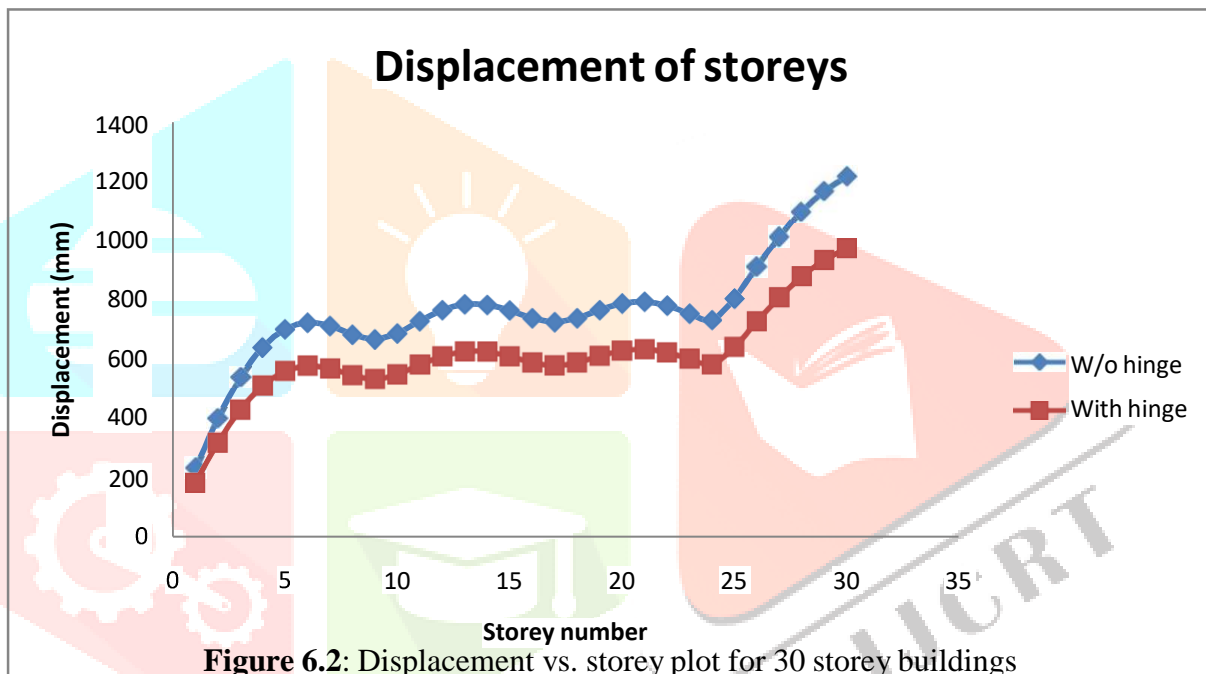
Table 6.1: Modal period and frequency of structure.

Modes	Period	Frequency
	(Second)	(Cycles/second)
1	3.87	0.26
2	3.87	0.26
3	3.366	0.30
4	1.26	0.79
5	1.26	0.79
6	1.12	0.89
7	0.71	1.41
8	0.71	1.41
9	0.66	1.51
10	0.50	2.00
11	0.50	2.00
12	0.47	2.13

6.2 Response of building with and without hinges.

6.2.1 Displacement plot

Figure 6.2 shows the graph between absolute displacement of joints of each storey for the case of explosion with the standoff distance 10 m and charge weight of 1000kg TNT. Two cases were taken, structure with hinges and without hinges. The hinges were provided at columns and beams. Storey number of both structures is 30. Front face was subjected to time history blast loads.



The displacement of top storey is maximum for both the cases. Due to application of hinge, the structure shows less deflection with respect to the structure without hinge. This is due to fact that with high strain rates, the strength of material increases. The structure with hinges gives better picture at the time of explosion as it gives more realistic results. For both the cases, the displacement values increases linearly till 7th floor and then becomes nearly linear and again it increases sharply. The difference in maximum displacements is nearly 300mm. In each of the case, constant difference in displacement value was observed.

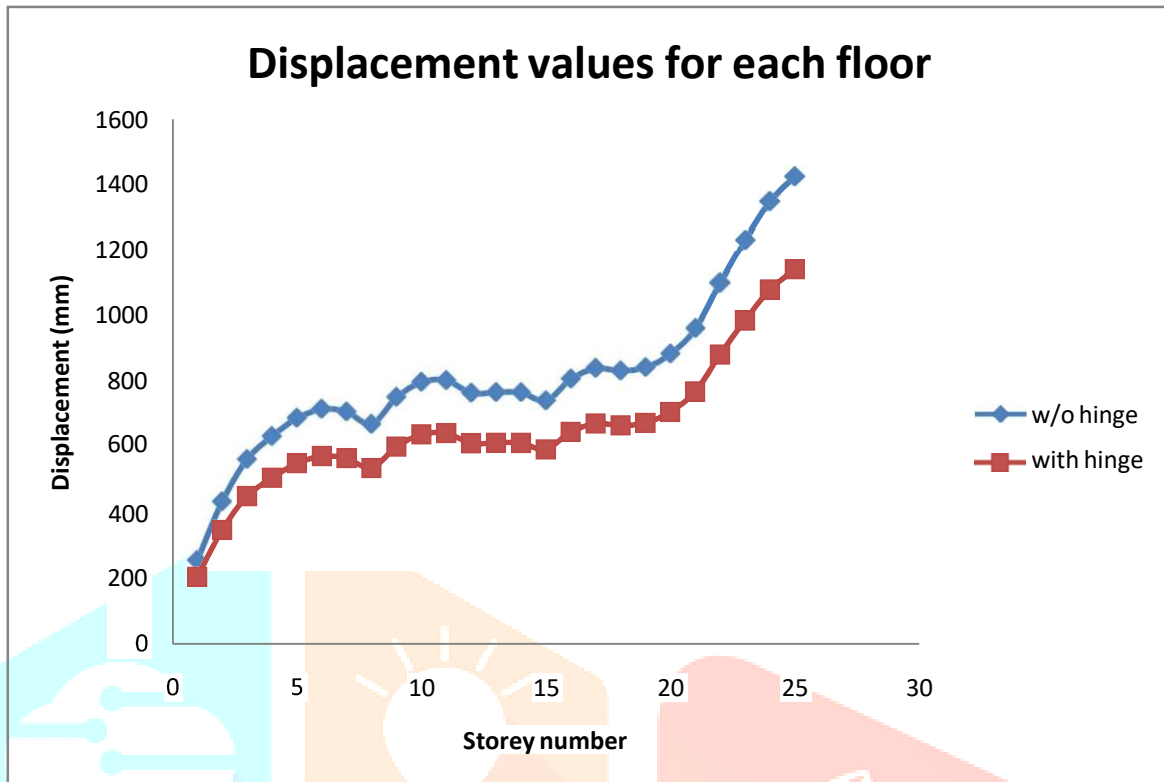


Figure 6.3: Displacement vs. storey plot for 25 storey buildings

Figure 6.3, 6.4, 6.5, 6.6 and 6.7 shows the plot of displacement vs. storey number for the case of twenty five, twenty, fifteen, ten and five storey's respectively. The results are compared with the structures with hinges for same storey numbers. Nearly all the graphs show the same variation of displacement with storey number. Top floor displacement is maximum for all the cases. For all the cases, structure with hinges shows realistic values that is less displacement values. In all the cases the difference in maximum displacement is also nearly same.

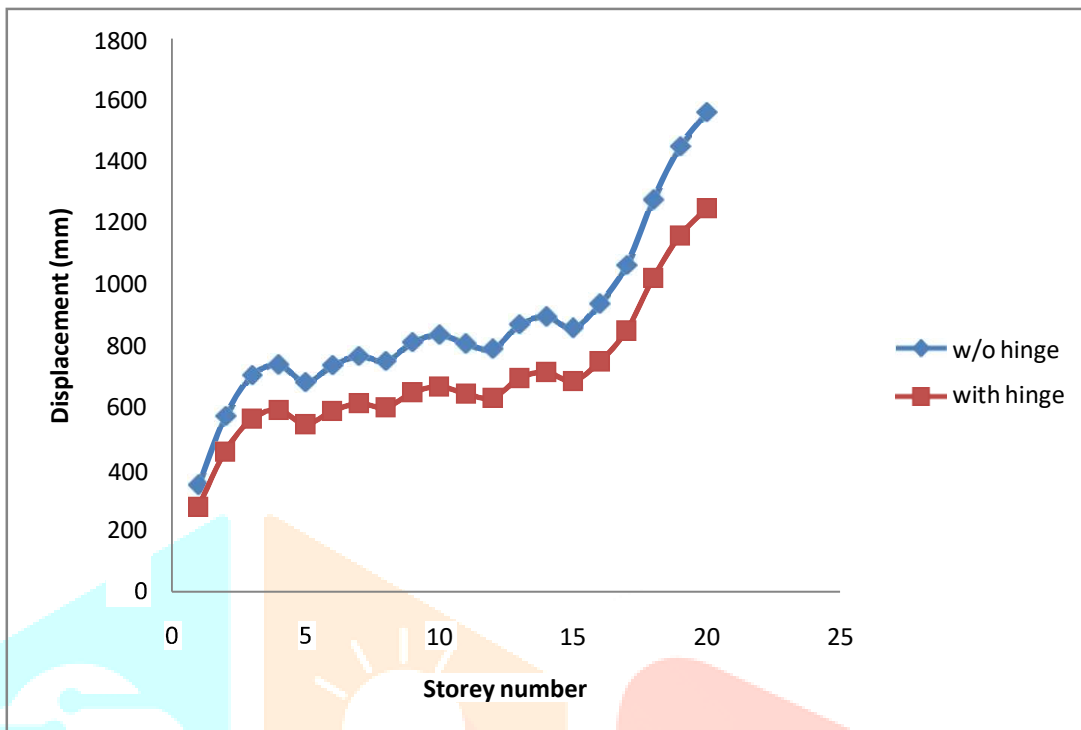


Figure 6.4: Displacement vs. storey plot for 20 storey buildings

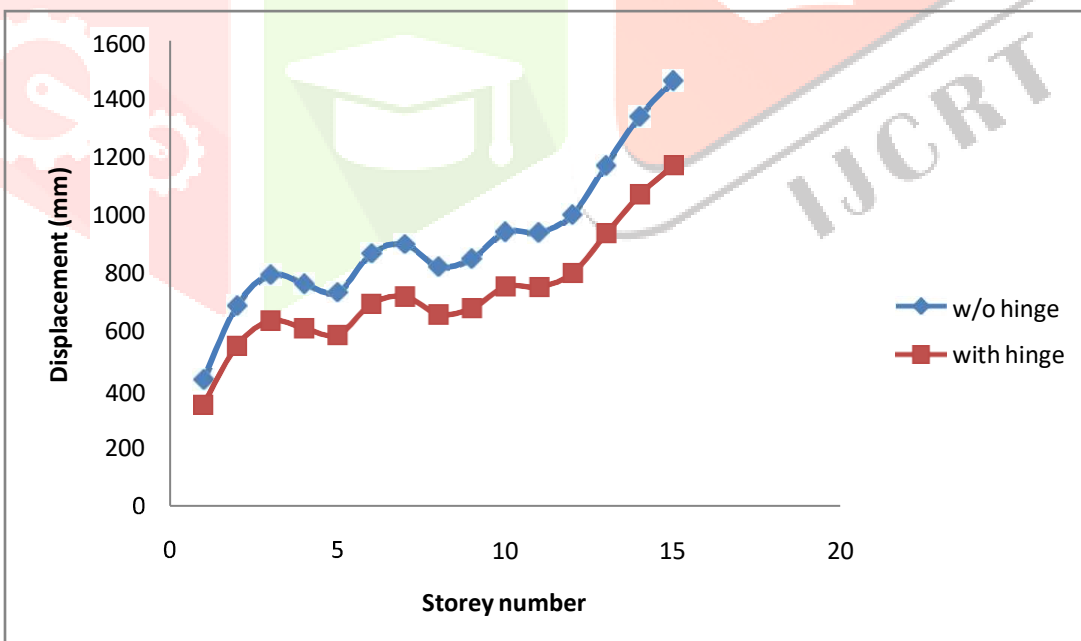


Figure 6.5: Displacement vs. storey plot for 15 storey buildings

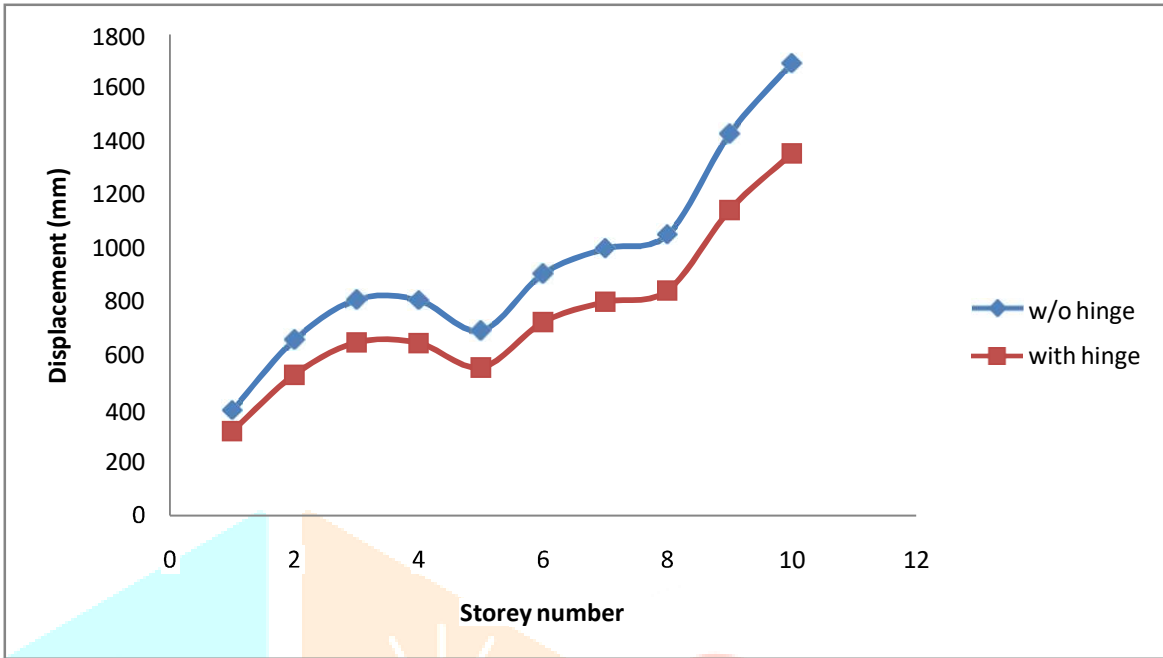


Figure 6.6: Displacement vs. storey plot for 10 storey buildings

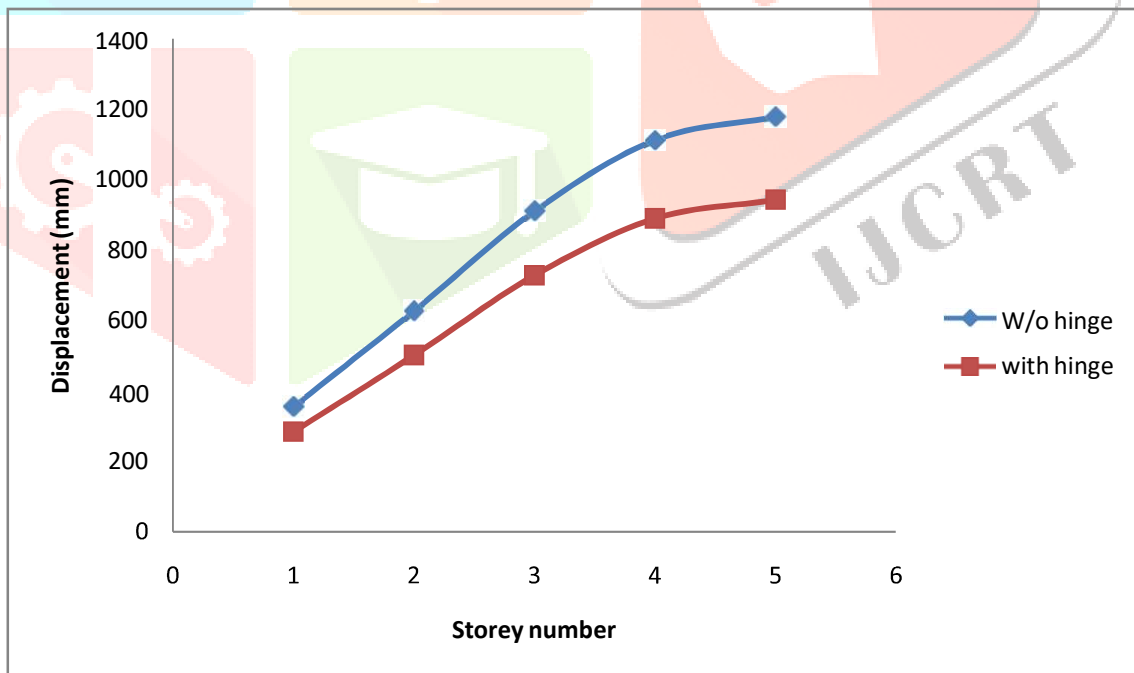
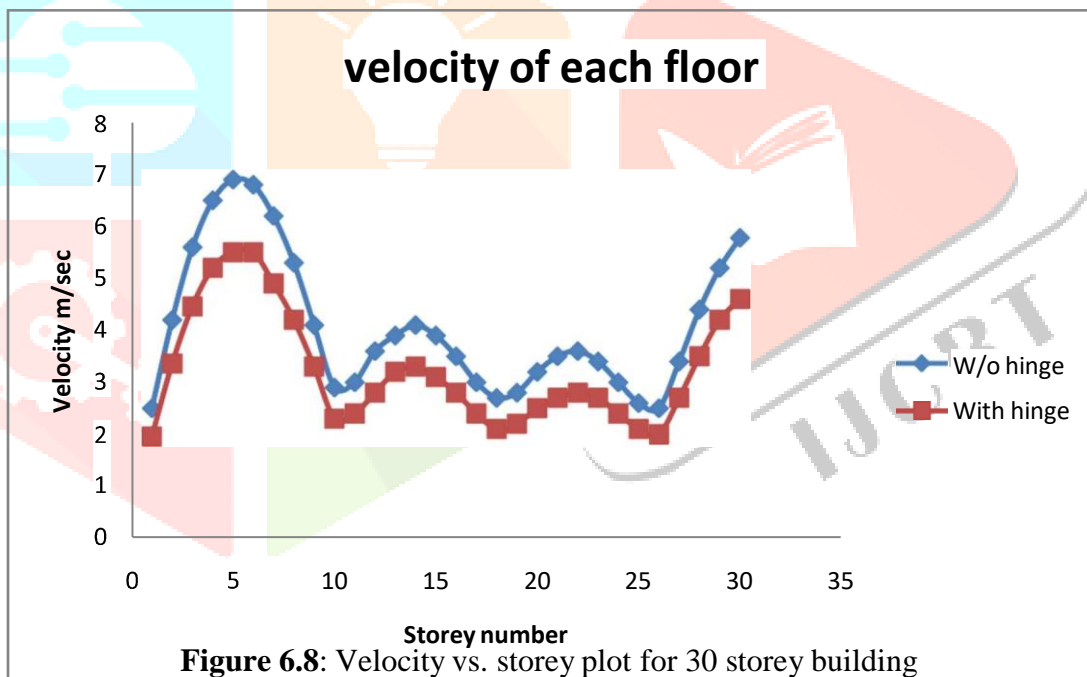


Figure 6.7: Displacement vs. storey plot for 5 storey buildings

6.2.2 Velocity plot

Figure 6.8 shows the plot of joint velocity with storey number. The structure with hinges shows less joint velocity as compared to structure without hinges. Joint velocity increases with increase in number of storey till 5th storey. Some local maxima's occurs between floor 5th and 22nd. The maximum joint velocity occurs at 5th floor for both the cases. Then it starts decreasing till 10th floor .then it increases and decreases till 22nd floor. After that it linearly increases till 30th storey. Similar curves were obtained for 25, 20, 15, 10 and 5 storey's as shown in Figure 6.9 to figure 6.13. The difference is that peak velocity occurs at top floor of these 5 structures. Structures with less storey number shows less local maxima's. The curve also becomes smoother as number of storey's decreased.



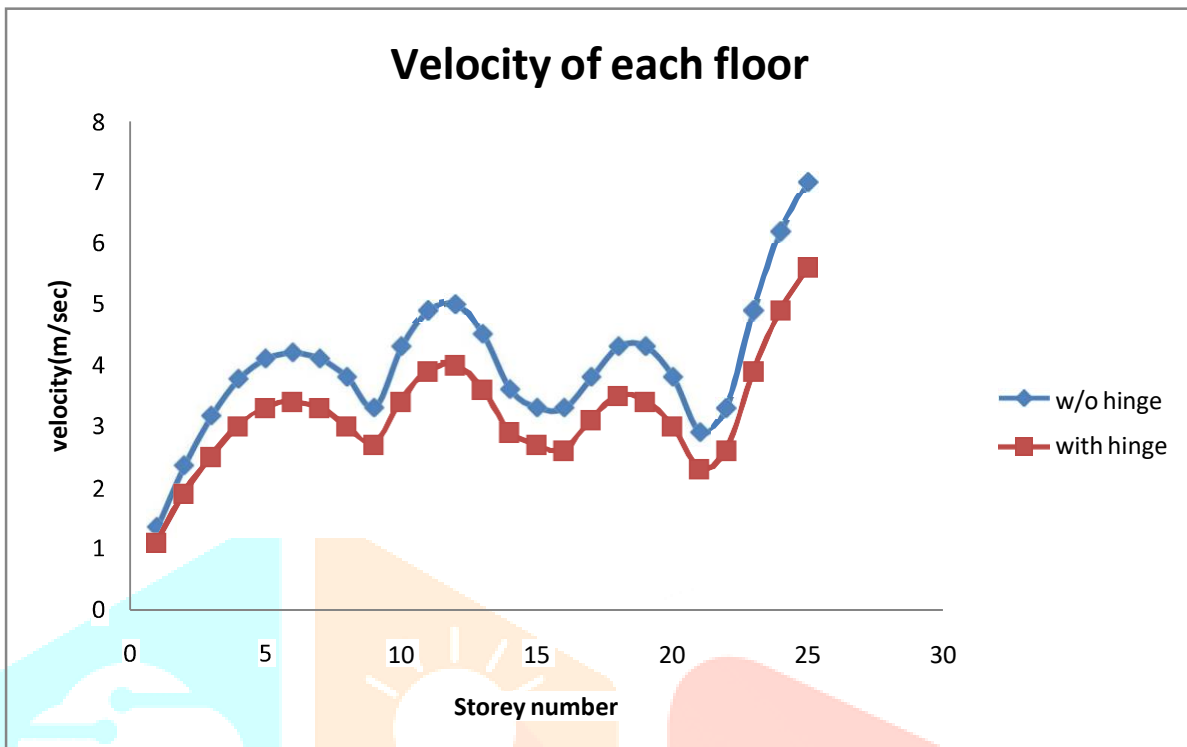


Figure 6.9: Velocity vs. storey plot for 25 storey building

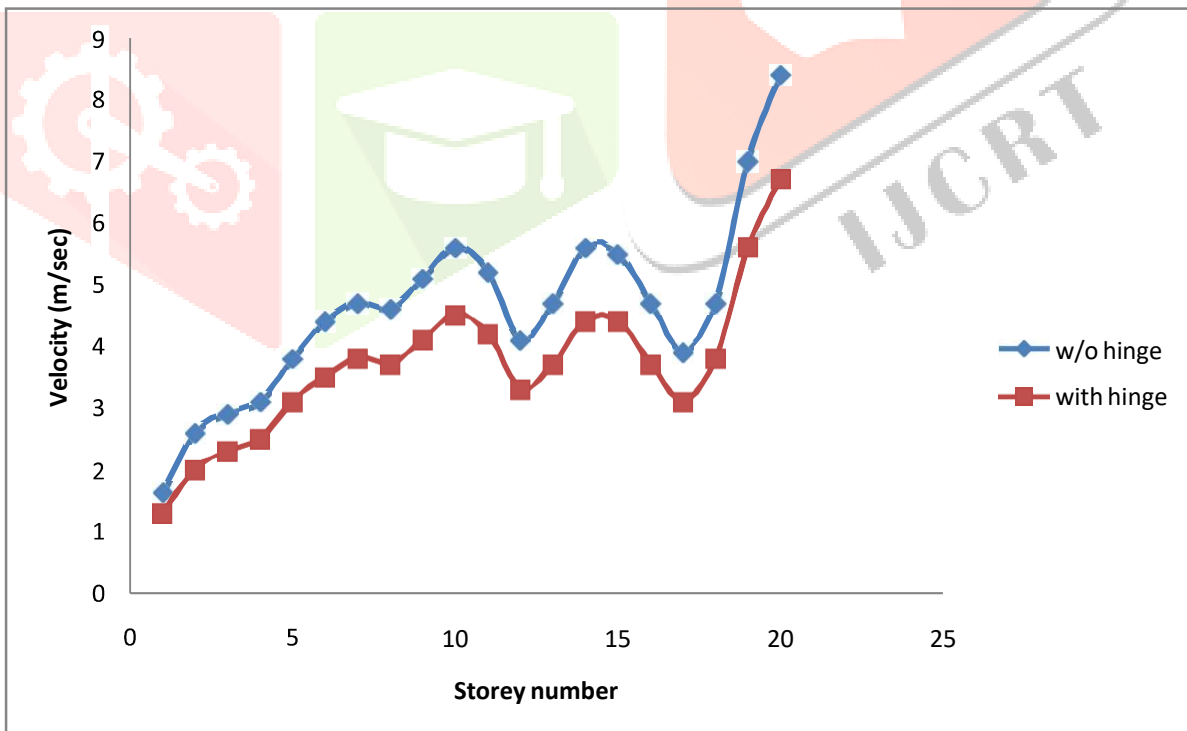


Figure 6.10: Velocity vs. storey plot for 20 storey building

For structures with five storeys, the curve is nearly horizontal till 4th floor. Maximum occurs at 5th floor. It can also be seen that top storey displacement increases with decrease in number of storey of structure. The maximum top storey joint velocity occurs on structure with five storey. Blast loading is a kind of lateral loading. The weight of structure provides stiffness to the structure. If the weight of the structure is more, then it provides more resistance to lateral loads. Due to this, joint velocity increases with decrease in storey number.

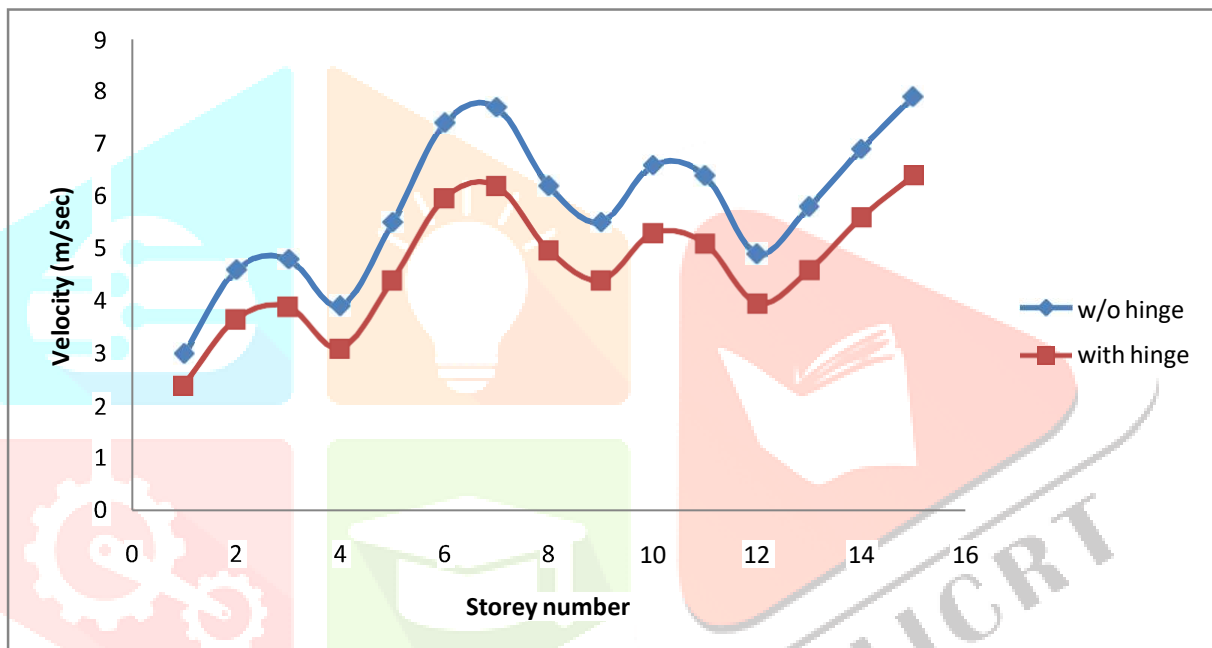


Figure 6.11: Velocity vs. storey plot for 15 storey building

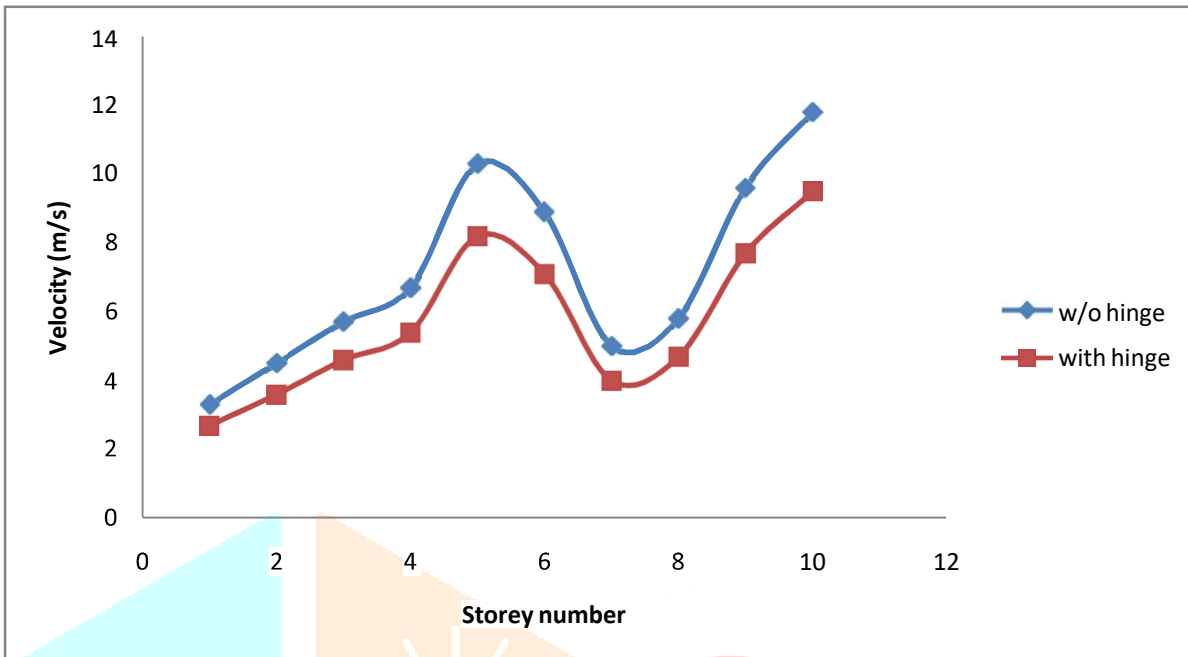


Figure 6.12: Velocity vs. storey plot for 10 storey building

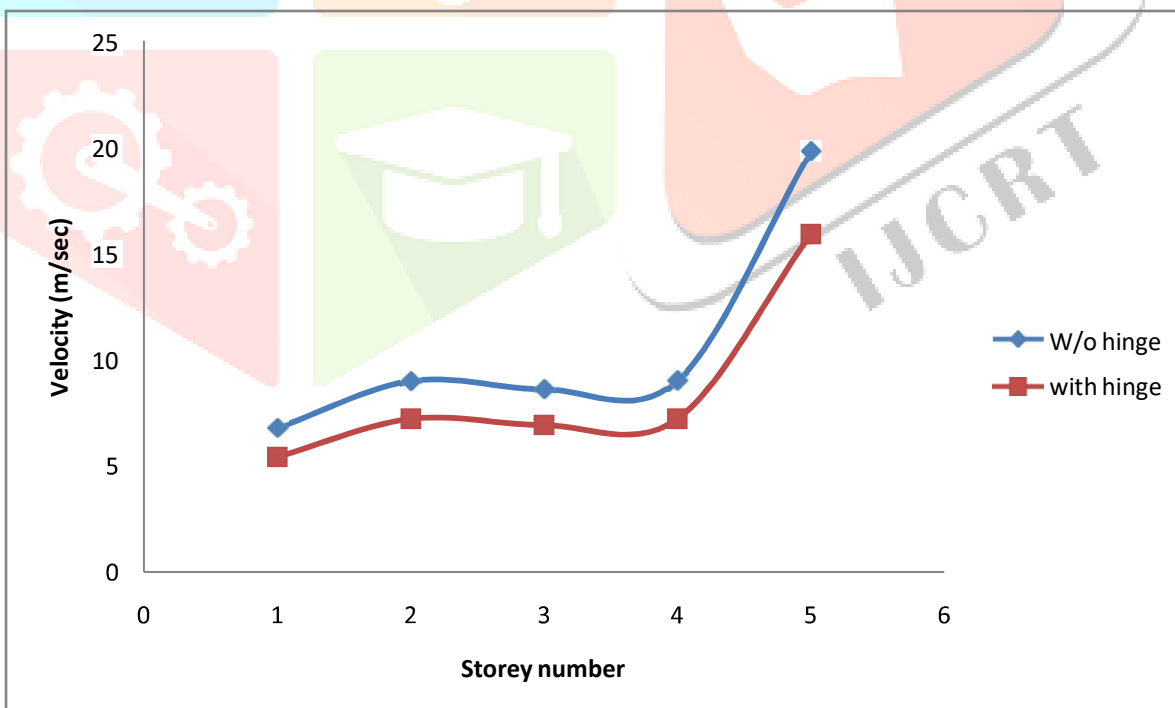
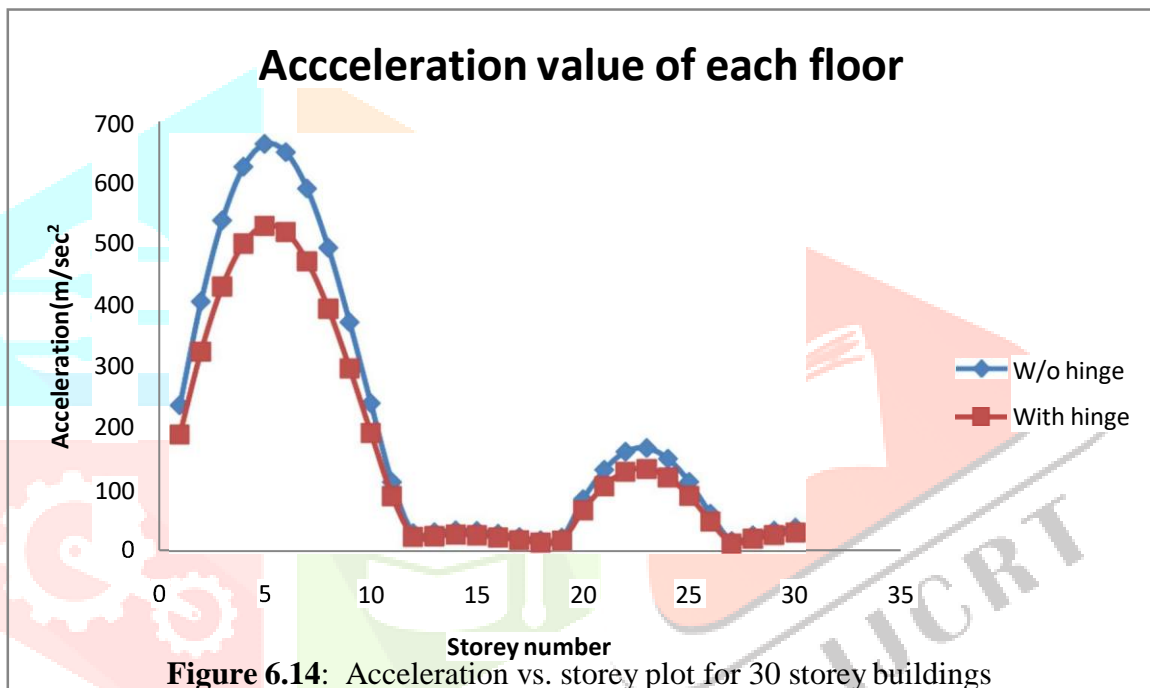


Figure 6.13: Velocity vs. storey plot for 5 storey building

6.2.3 Acceleration plot

Figure 6.14 shows the plot of joint acceleration for each storey for the case of structure with and without hinges. The buildings are of 30 storey. The joint acceleration value increases instantaneously till 5th floor joint, and then its value starts reducing. After 12th floor the value becomes nearly constant till 20th storey. Again its value increases but with less rate, with a local maximum value occurring at 23rd storey. After that, it reduces to minimum value at 27th storey. After 27th storey its value starts increasing.



Similar trend also occurred for storey without hinge. The structure with hinges at beams and columns provides less joint acceleration value when compared with the structures without having hinges. The maximum joint acceleration value is about 680 and 540 m/sec², which occurred at 5th floor for the structure without hinge and with hinge respectively.

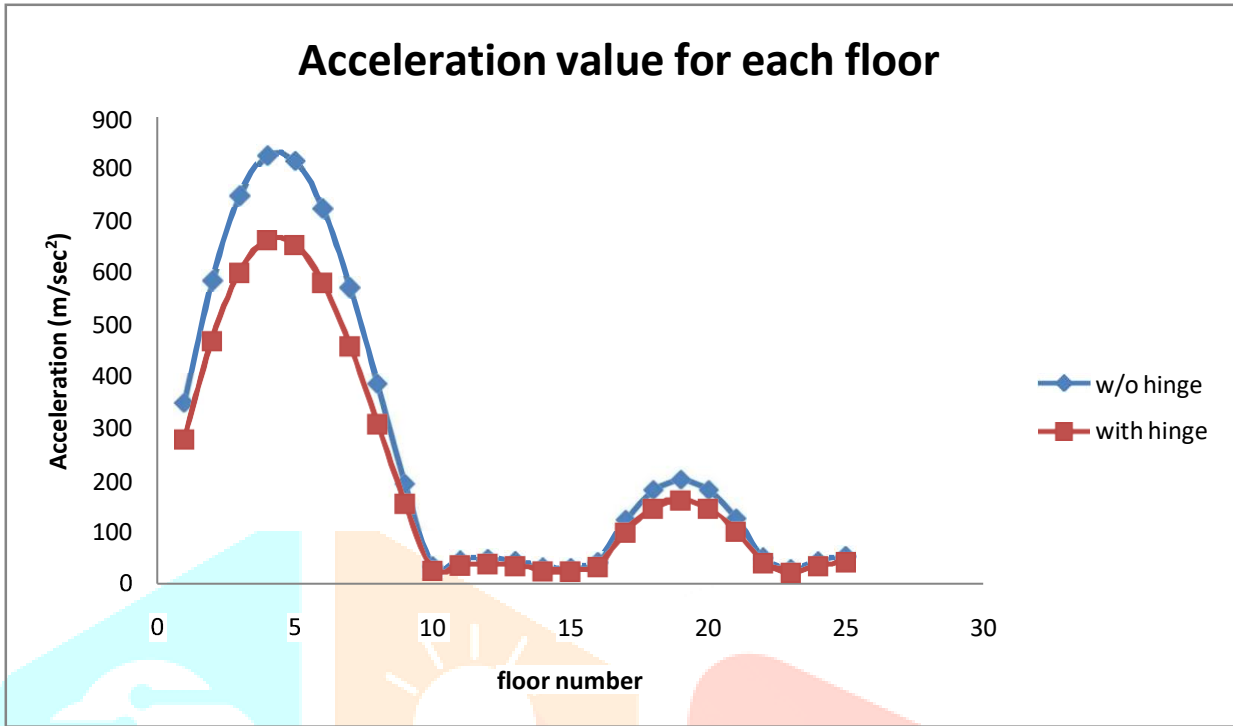


Figure 6.15: Acceleration vs. storey plot for 25 storey buildings

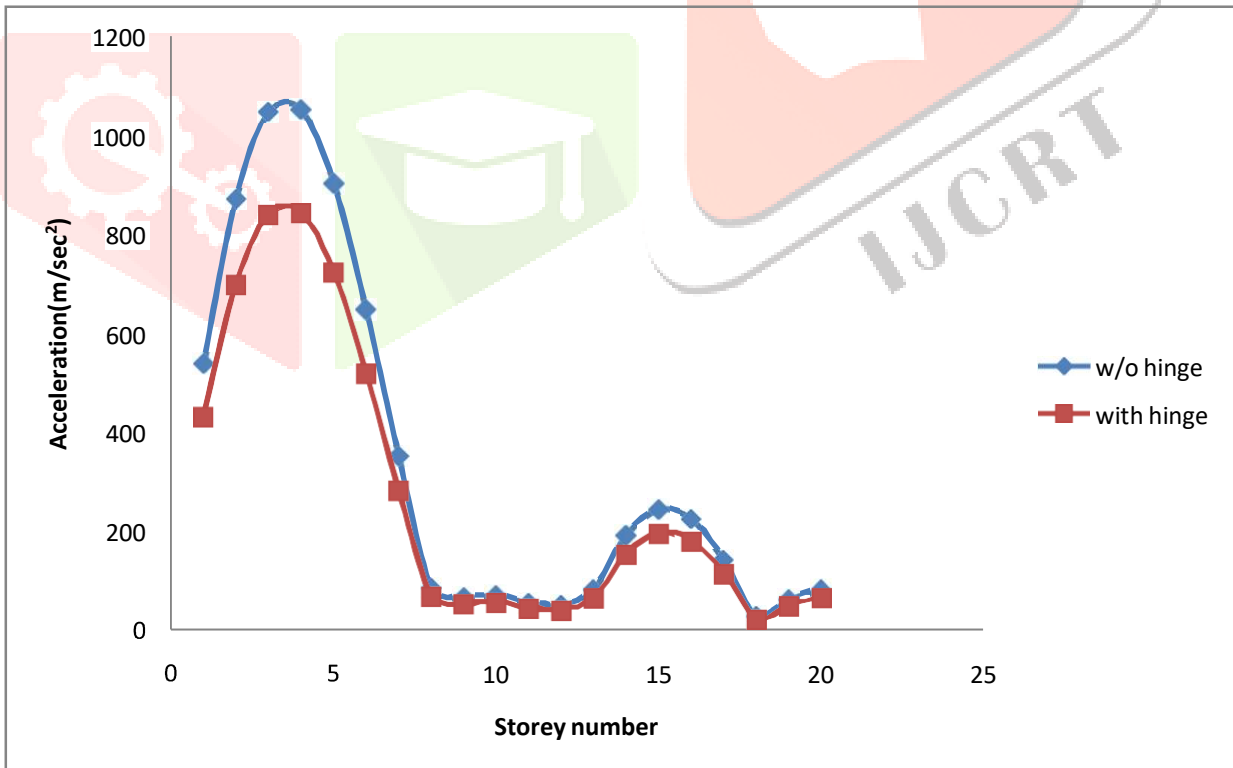


Figure 6.16: Acceleration vs. storey plot for 20 storey buildings

Figure 6.15 to figure 6.19 also shows the plot of joint acceleration of each floor for 25, 20, 15, 10, and 5 storey buildings. Two cases were analyzed for each building that is, the structure with hinge and without hinges. In all the cases, the structure with hinge showed less joint acceleration values. The maximum joint acceleration value increases with decrease in structure height, that is the five storey structure had maximum joint acceleration followed by 10, 15 and so on.

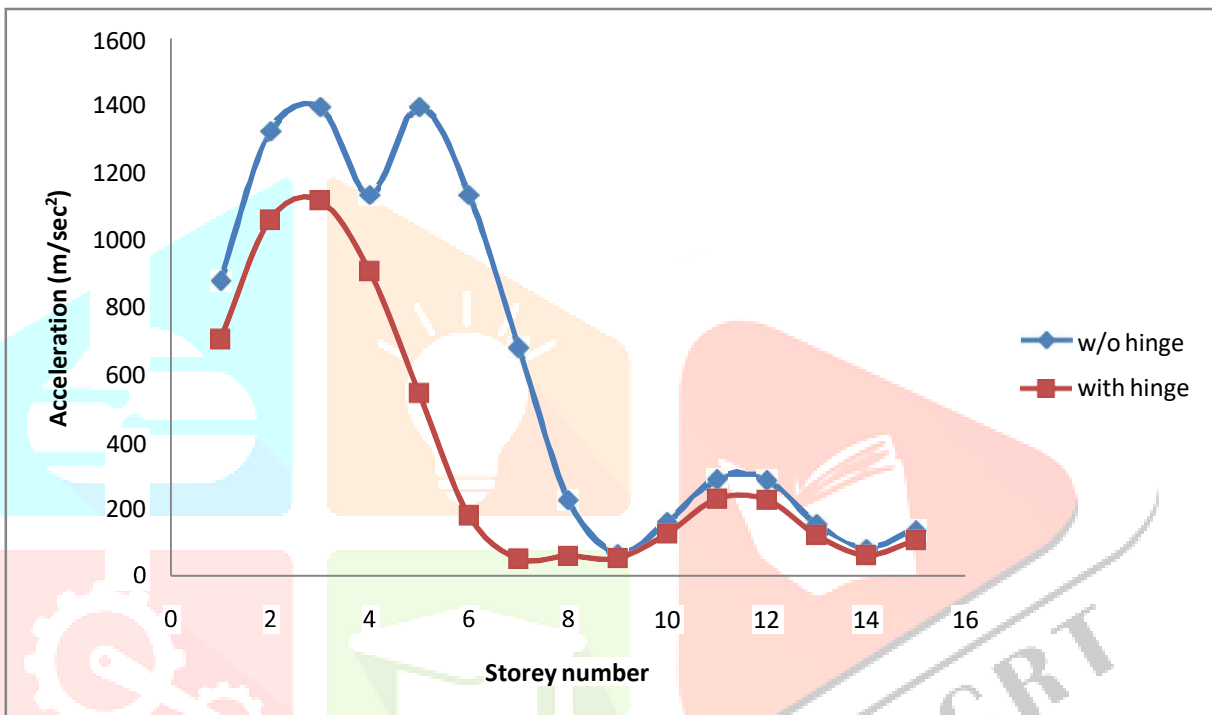


Figure 6.17: Acceleration vs. storey plot for 15 storey buildings

The peak joint acceleration occurred on first storey with the value of 2700m/sec^2 and 2100m/sec^2 for five storey building without hinge and hinge respectively. Its peak acceleration value occurred at high storey levels as the structure height increases. This is due to fact that maximum joint load value occurred at lower storeys with less value at higher storeys. That is why the peak acceleration occurred at 5 storey structure. Also the structure with hinge showed less response when compared with structure without hinges.

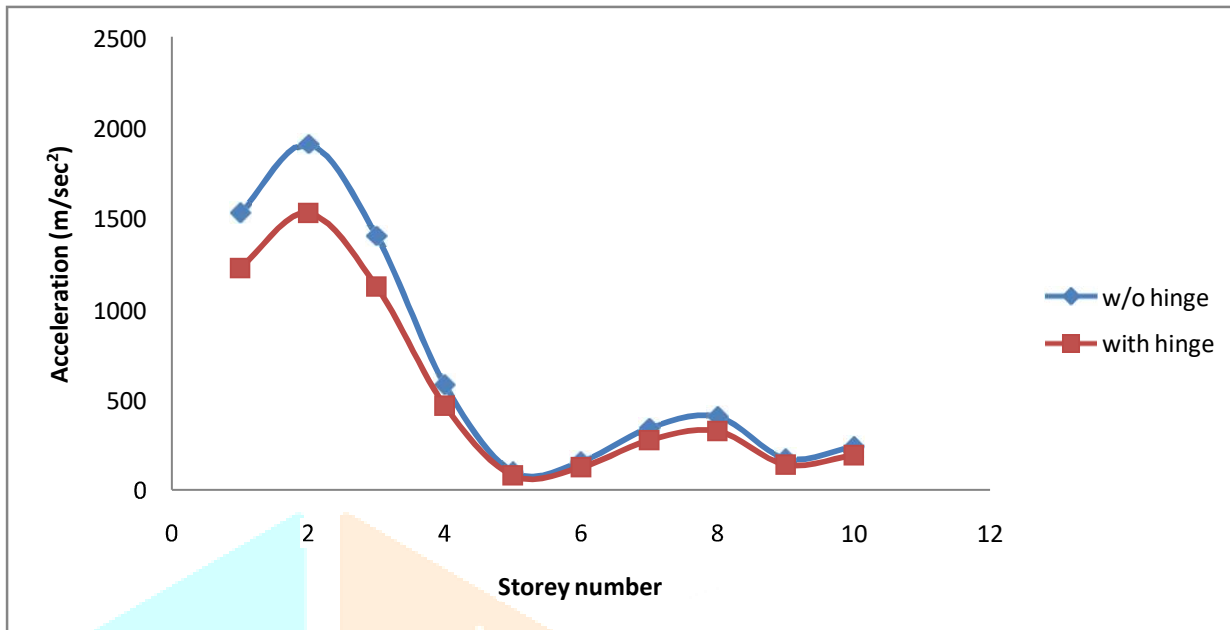


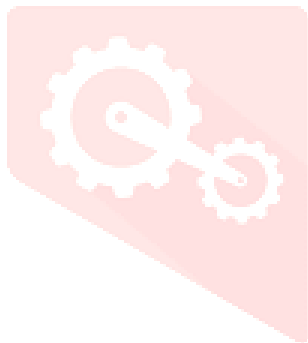
Figure 6.18: Acceleration vs. storey plot for 10 storey buildings



Figure 6.19: Acceleration vs. storey plot for 5 storey buildings

So, by comparing the structural response with and without hinge, we may conclude that by application of hinge, we can get more clear picture of structural response. Displacement, velocity and acceleration of joints were less for the case of structure without hinge and vice versa.

It was also seen that the response of structures with less storey was more than that on structure with higher storey's. As we know that the peak pressure of blast load depends on standoff distance. If the point of detonation is more, the pressure will be less. The overpressure value reduces exponentially with increase in standoff distance. Therefore joint load value is maximum for first floor and it decreases as the number of storey increases. Maximum blast forces are concentrated in lower number of storey's only. Due to this, the net blast force subjected by structure with five storey varies by a small amount when compared with structures with more number of storey's. We also know that weight of structure increases its stiffness. Therefore more number of storey's implies more resistance against lateral loads. So, we may conclude that building with less height is more vulnerable to blast loading. Also from joint load calculations, we come to know that the interior columns takes majority of blast loads. So, to resist these large time dependent loads, the interior columns should be made more strong and stiffer. This can be done by increasing the size of columns.



6.3 Variation of response with change in stand-off distance.

In the second part of analysis, the variation of structural response with change in stand-off distance is presented. Two stand-off distances of 10m and 5m were used for the analysis. The explosive used was 1000kg for both the cases. The storey number of the buildings was 30m, 25m, 20m, 15m, 15m, 10m and 5m for both the cases. Hinges were provided on beams and columns for both the cases. Figure 6.20 shows the variation of displacement of storey's for both the cases of stand-off distance.

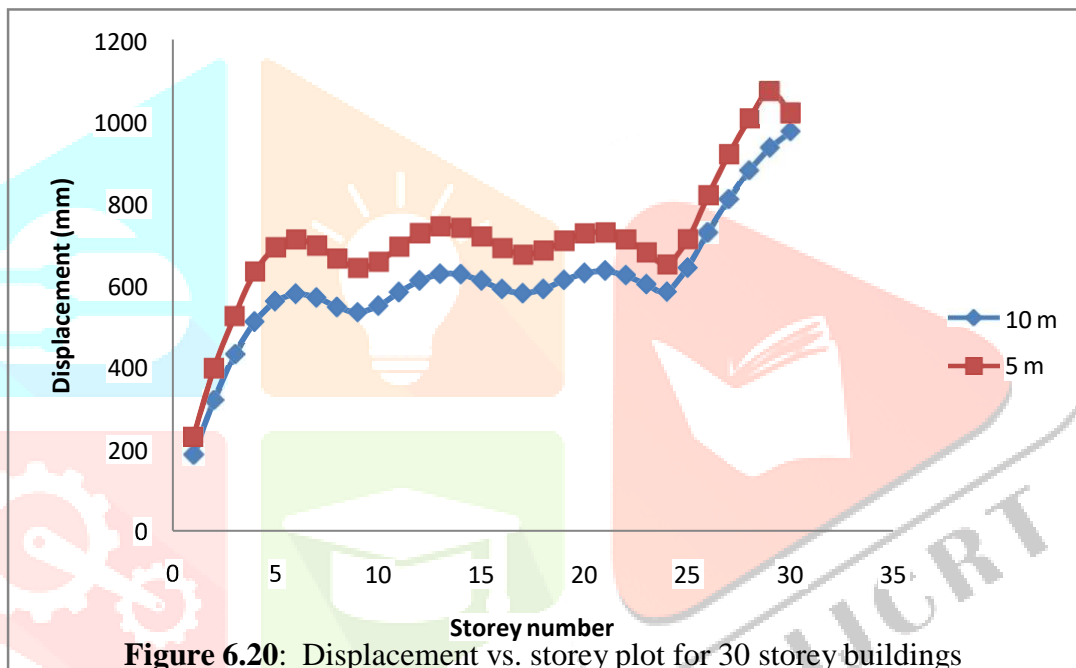


Figure 6.20: Displacement vs. storey plot for 30 storey buildings

The joint displacement for the case of 5m stand-off displacement is more for each storey's when compared with 10 m stand-off distance. The displacement values increases linearly till 6th floor then becomes nearly linear and again increases linearly from 25th floor till top floor. The minimum displacement value is 220mm for the case of 5 m stand-off distance. Similar trend is followed for the case of 10 m stand-off distance also.

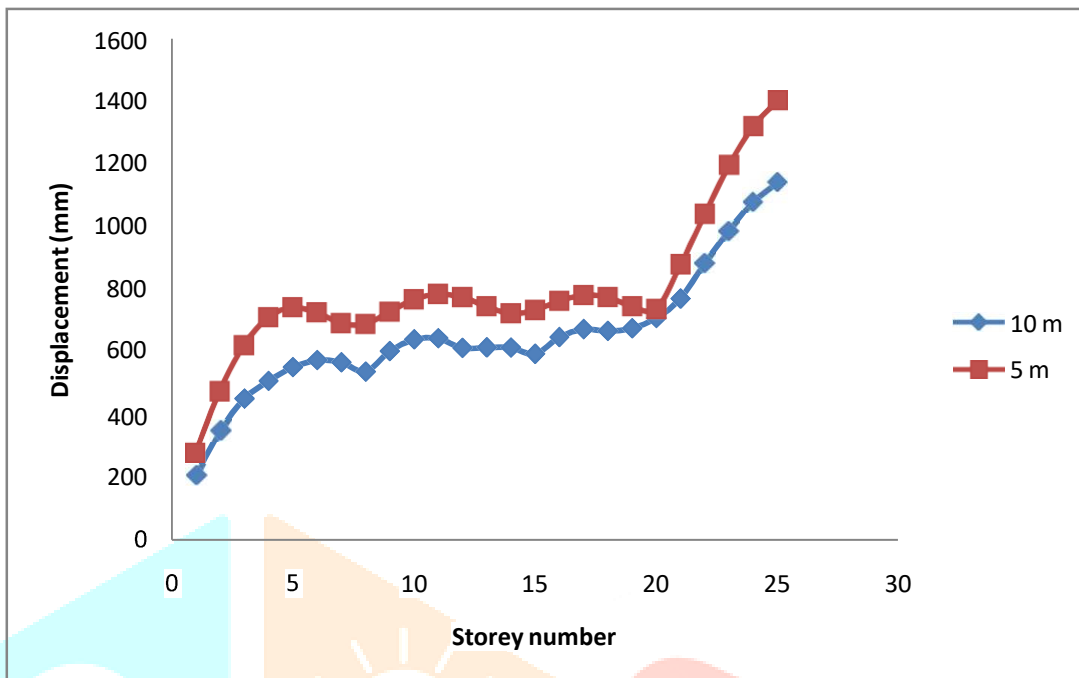


Figure 6.21: Displacement vs. storey plot for 25 storey buildings

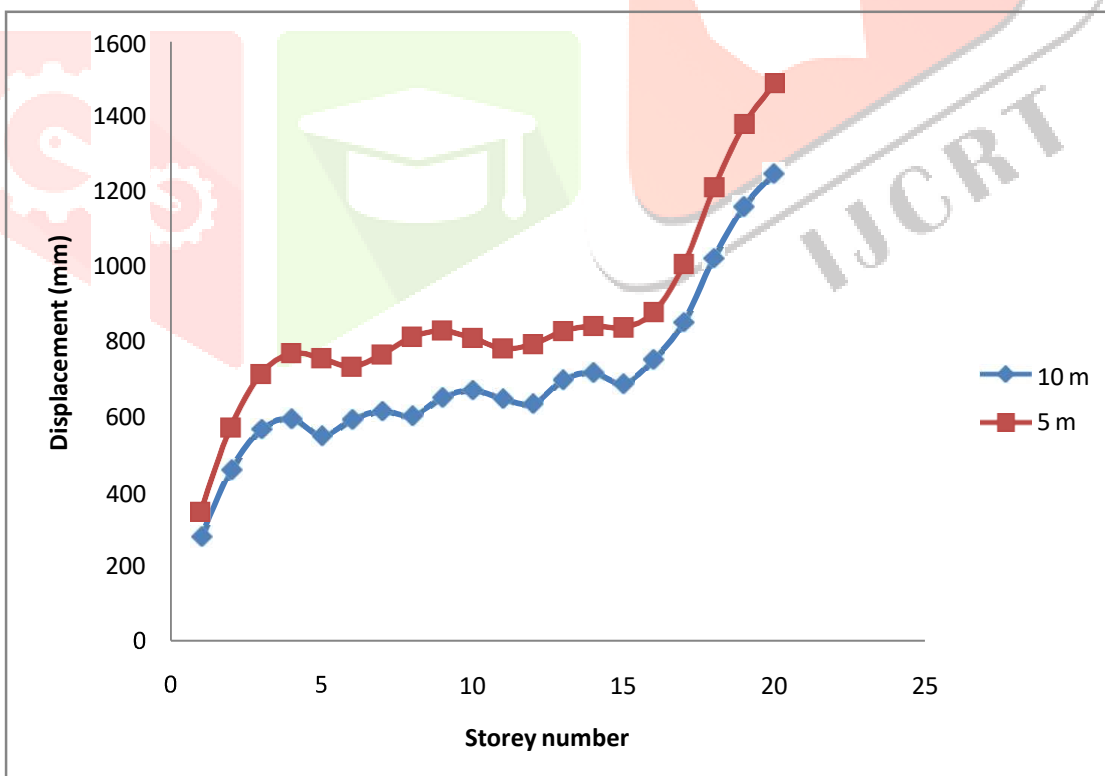


Figure 6.22: Displacement vs. storey plot for 20 storey buildings

Figure 6.21 to figure 6.25 shows the joint displacement plot of each storey's for building with number of storey 25,20,15,10 and 5 respectively for both the case of 5m and 10 m stand-off distance respectively.

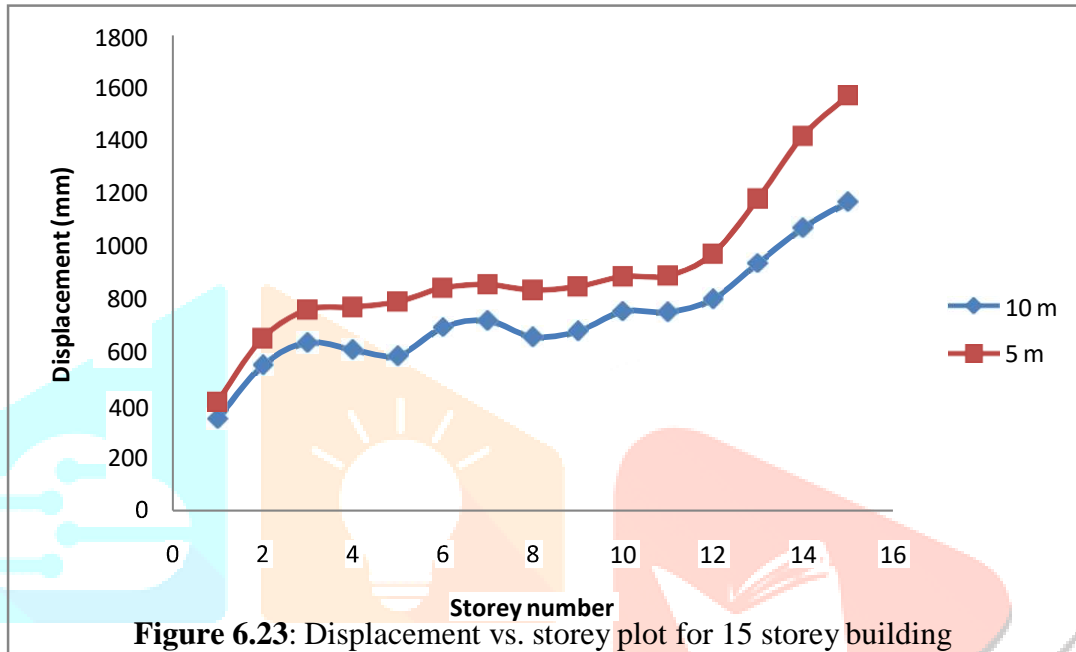


Figure 6.23: Displacement vs. storey plot for 15 storey building

For all the cases, joint displacement value is always more for the case of 5m stand-off distance. The difference in storey displacement value widens as the height of building reduces. Also first floor displacement value is more for 5 storey structures than the structure with more number of storey's. The displacement curve becomes smoother and linear as the height of building reduces. Blast loading is a kind of exponential loading. So varying stand-off distance by 5m, the load on joint increases by number of times.

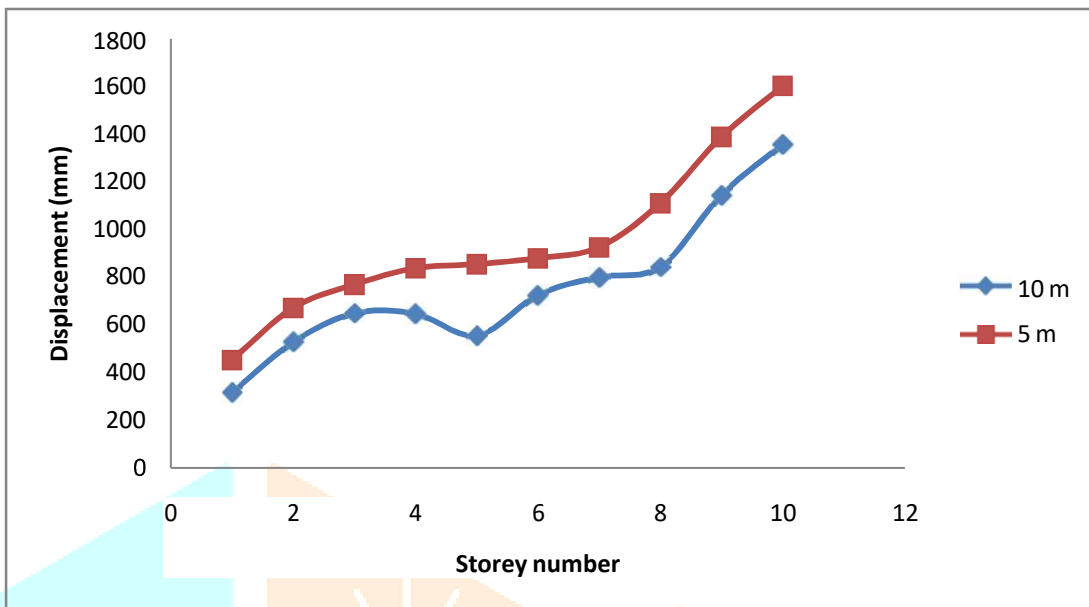


Figure 6.24: Displacement vs. storey plot for 10 storey buildings

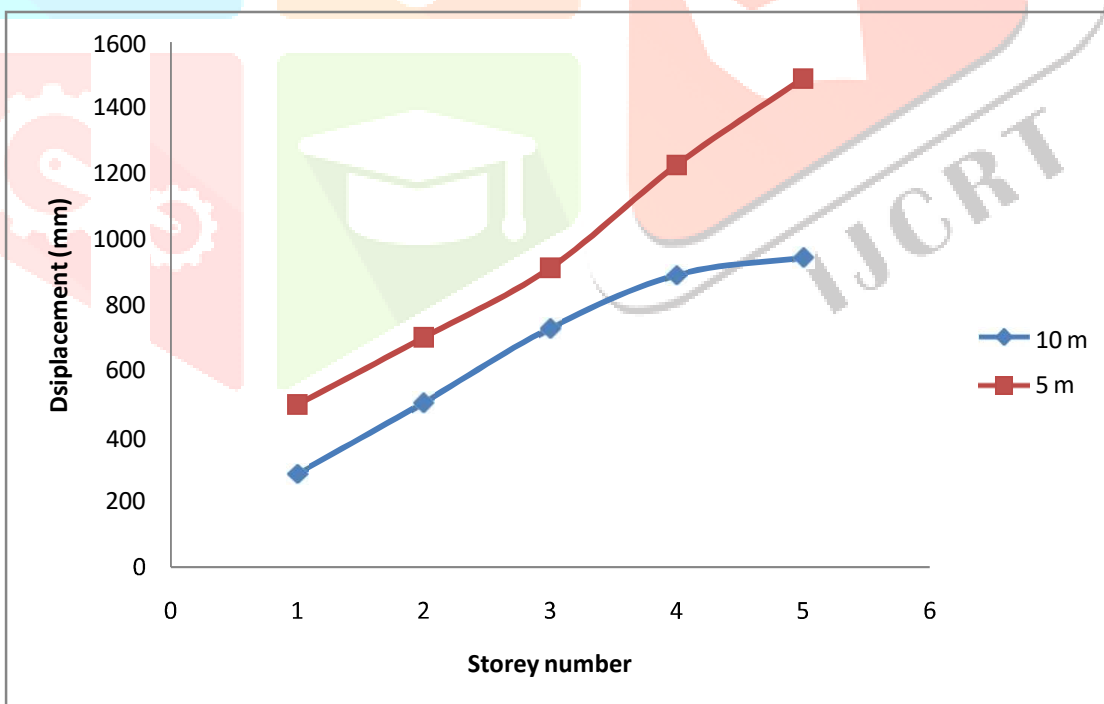


Figure 6.25: Displacement vs. storey plot for 5 storey buildings

Figure 6.26 shows the plot of velocity of each floor joint for the case of 30 storey building for stand-off distance of 10 m and 5 m. For the case of 5 m stand-off distance, the joint velocity increases till 5th floor, then it starts reducing till 10th floor. From 10th to 25th storey two local maxima's and minima's occurred. The maxima were on 14th and 22nd floor and minima occurred on 18th and 26th floor. After that the velocity of joint increased at higher rate till it reaches its maximum value at 30th floor. The maximum velocity occurred at 5th floor not on 30th floor.

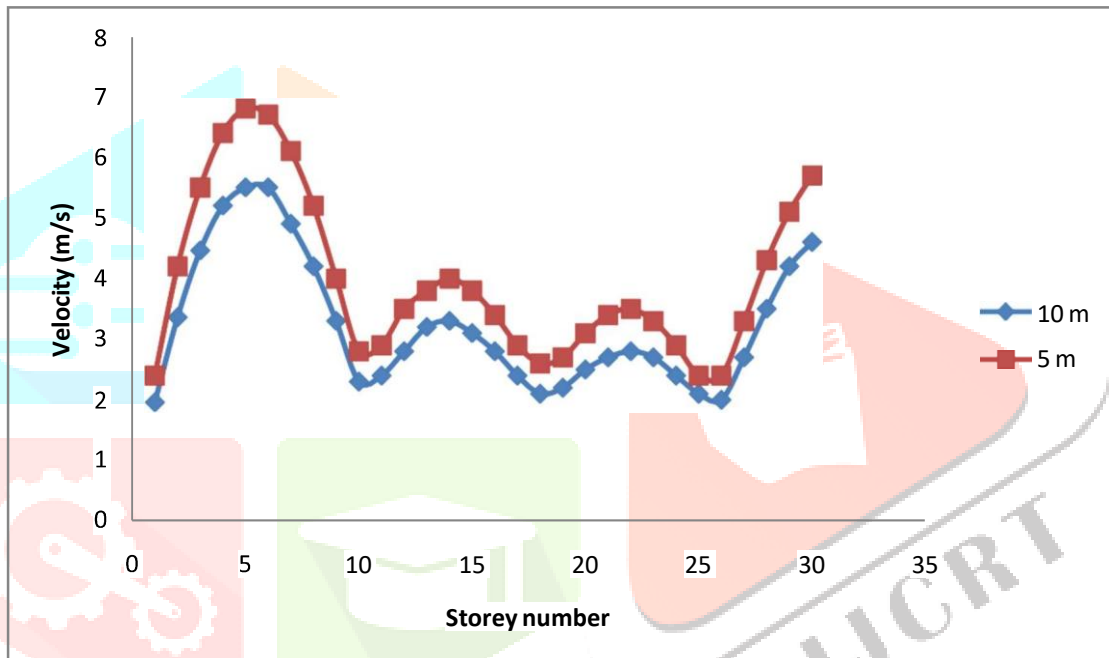


Figure 6.26: Velocity vs. storey plot for 30 storey building

The maximum joint velocity was 7 m/s. Similar trends were observed for stand-off distance of 10m also. The maximum joint velocity also occurred at 5th floor. The value was 5.8 m/s. minimum value of 2m/s occurred at 18th floor. The joint velocity value for each floor were always higher for 5 m stand-off distance.

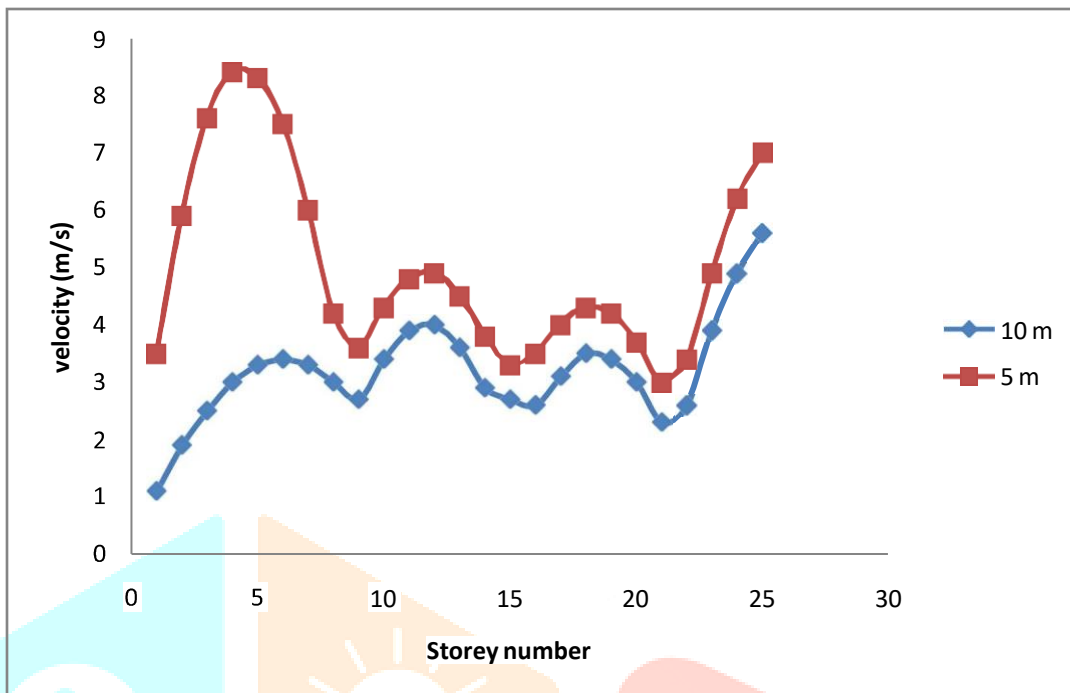


Figure 6.27: Velocity vs. storey plot for 25 storey building

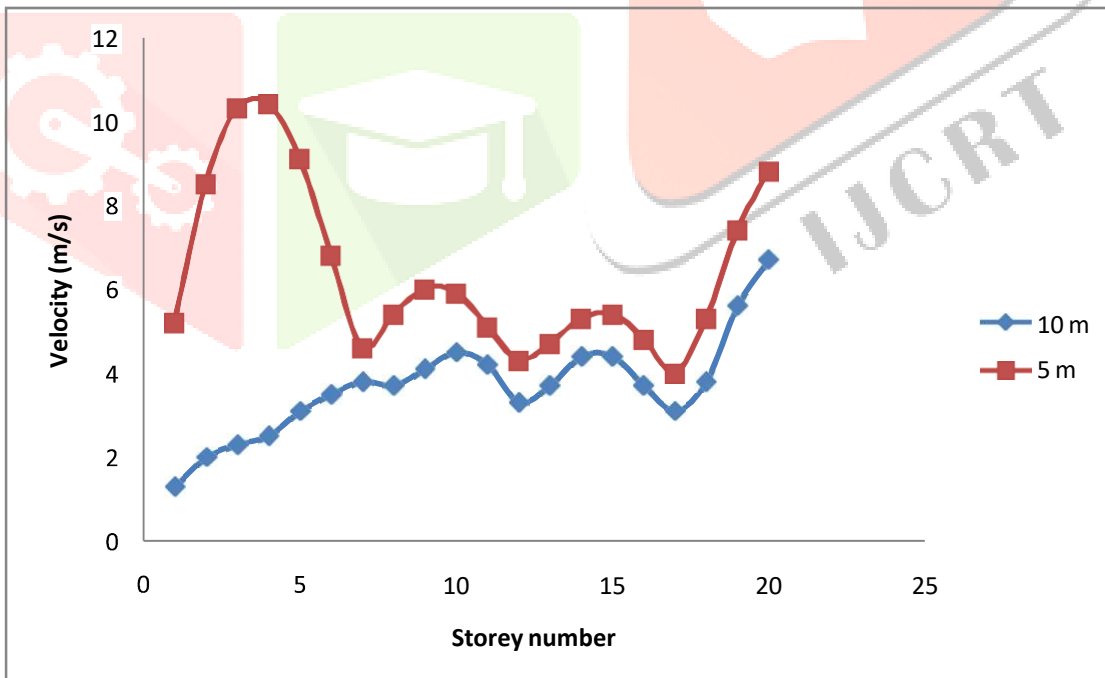
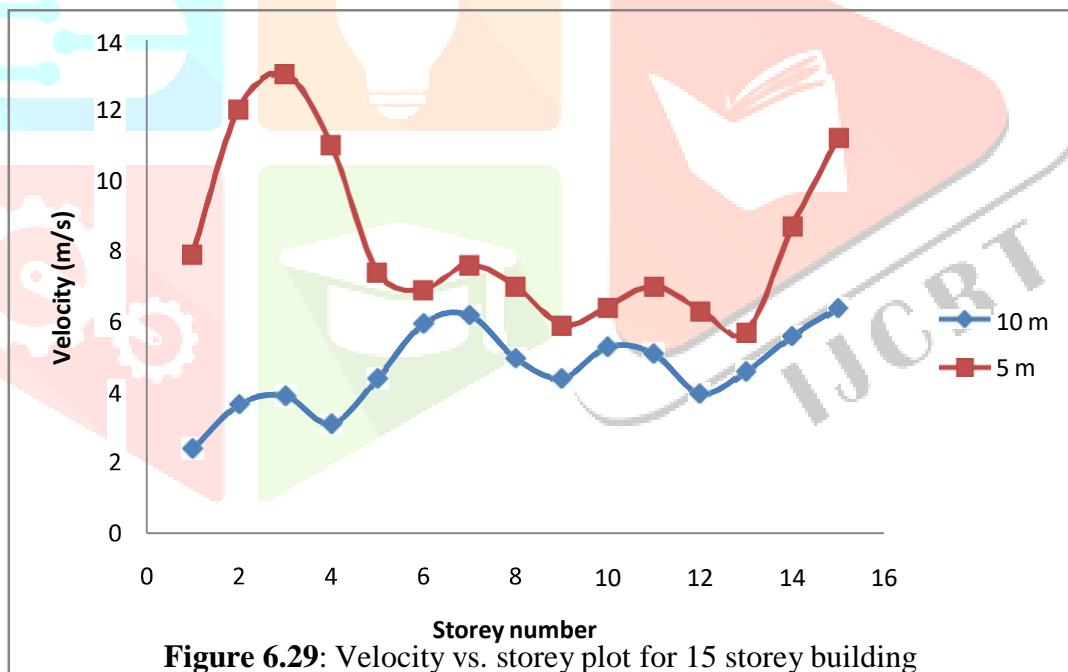


Figure 6.28: Velocity vs. storey plot for 20 storey building

Figure 6.27 to figure 6.31 shows the plot of joint velocity of each storey for 25, 20, 15, 10 and 5 storey building respectively. The joint velocity was maximum for 5th storey for all the building for 5m and 10 m stand-off distance. The second maxima also occurred at top floor for each building for both the cases. Also, when the stand-off distance was 5 m, each floor joint velocity was more when compared with the stand-off distance of 10 m. The building with less storey number yields more response. The maximum joint velocity of 5 storey building was more than all the buildings. As the storey height decreases, its joint velocity increases. The difference between local maxima and minima reduces with height of storey. The maximum joint velocity of 5th storey building was 17 m/s for stand-off distance of 5 m. The difference in joint velocity for both the cases of stand-off distance increases as the height of storey increases. This is due to fact that blast load is basically an exponential function of stand-off distance.



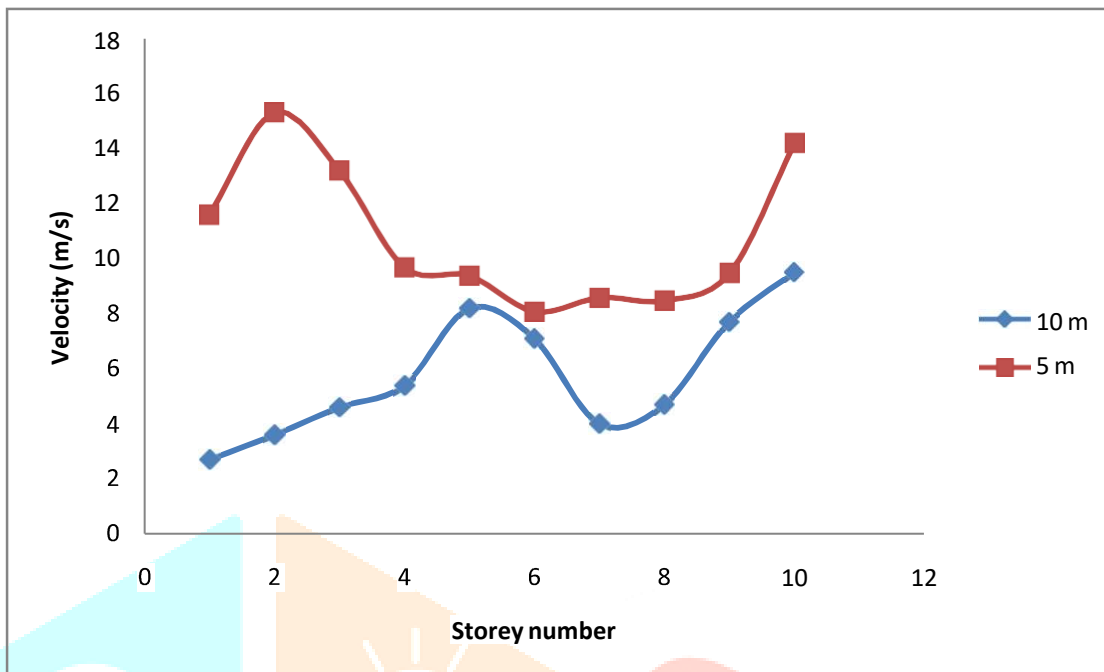


Figure 6.30: Velocity vs. storey plot for 10 storey building

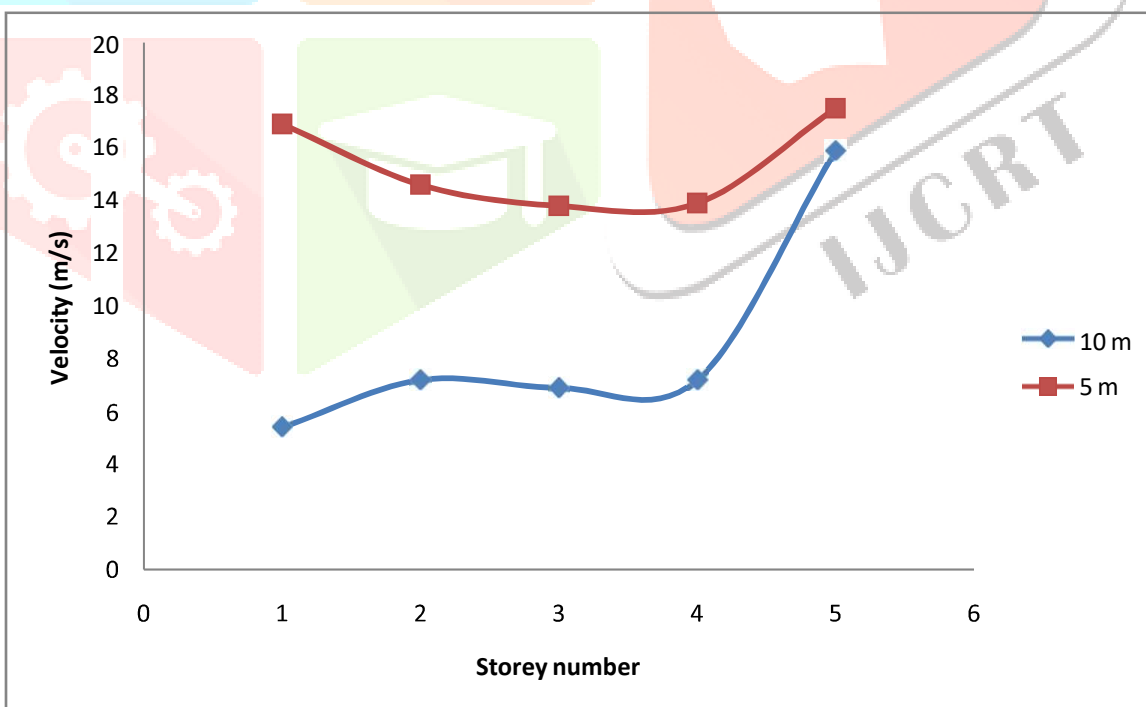


Figure 6.31: Velocity vs. storey plot for 5 storey building

Figure 6.32 shows the plot of joint acceleration value of each floor of a 30 storey RC building. Two cases were analyzed by varying stand-off distance. The stand-off distance of 10m and 5 m were used for calculation of loads. The joint acceleration value increases from first floor to 5th floor where maximum value of joint acceleration was observed. After 5th floor, the joint acceleration value starts reducing till 12th floor. From 12th to 20th floor the joint acceleration value is nearly same. Again after this, the value starts increasing till it reaches a smaller peak value at 23rd floor, then again it reduces. After 27th floor, the value starts increasing but with smaller rate.

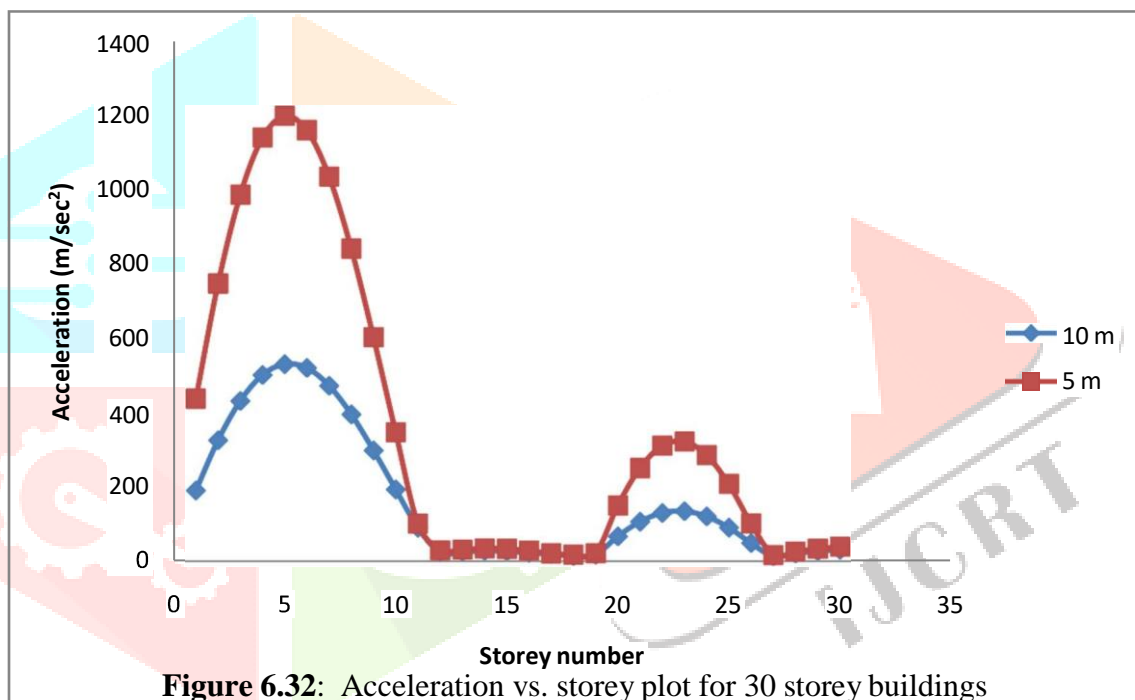


Figure 6.32: Acceleration vs. storey plot for 30 storey buildings

When the stand-off distance was 5m, the maximum joint acceleration occurred was 1200m/sec². The maximum joint acceleration for the case of 10 m stand-off distance was about 500m/sec². The difference in maximum acceleration value was relatively large. From 10th to 20th floor, the value was nearly same. In no case, the joint acceleration of the structure having point of detonation 10 m was more than the structure having stand-off distance 10 m.

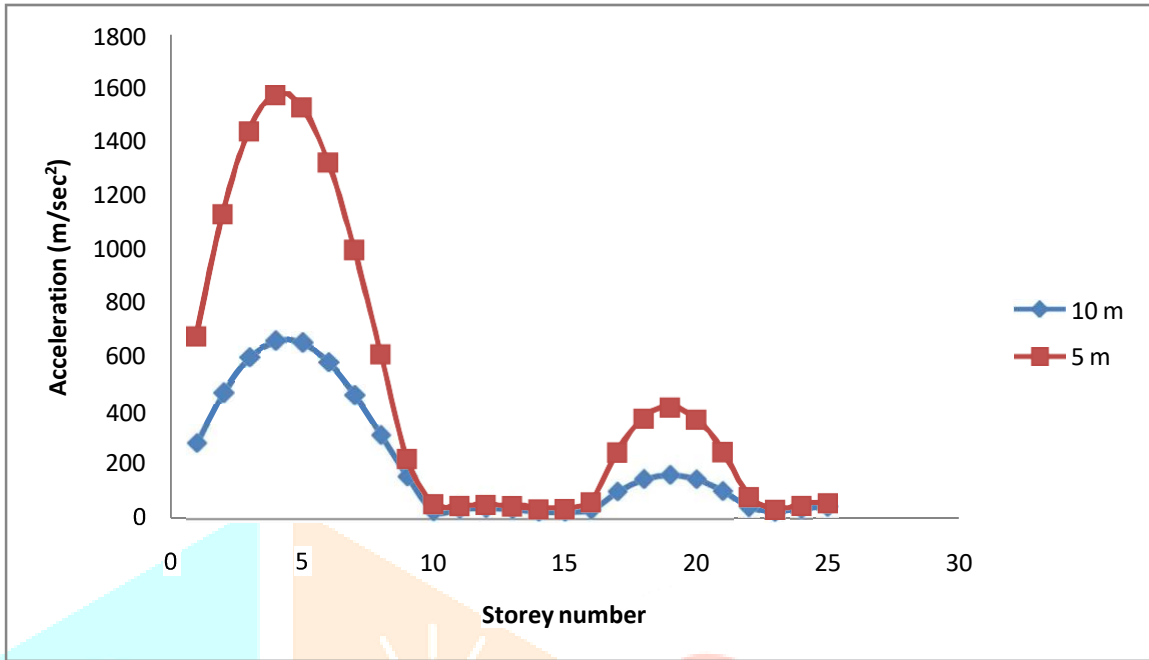


Figure 6.33: Acceleration vs. storey plot for 25 storey buildings

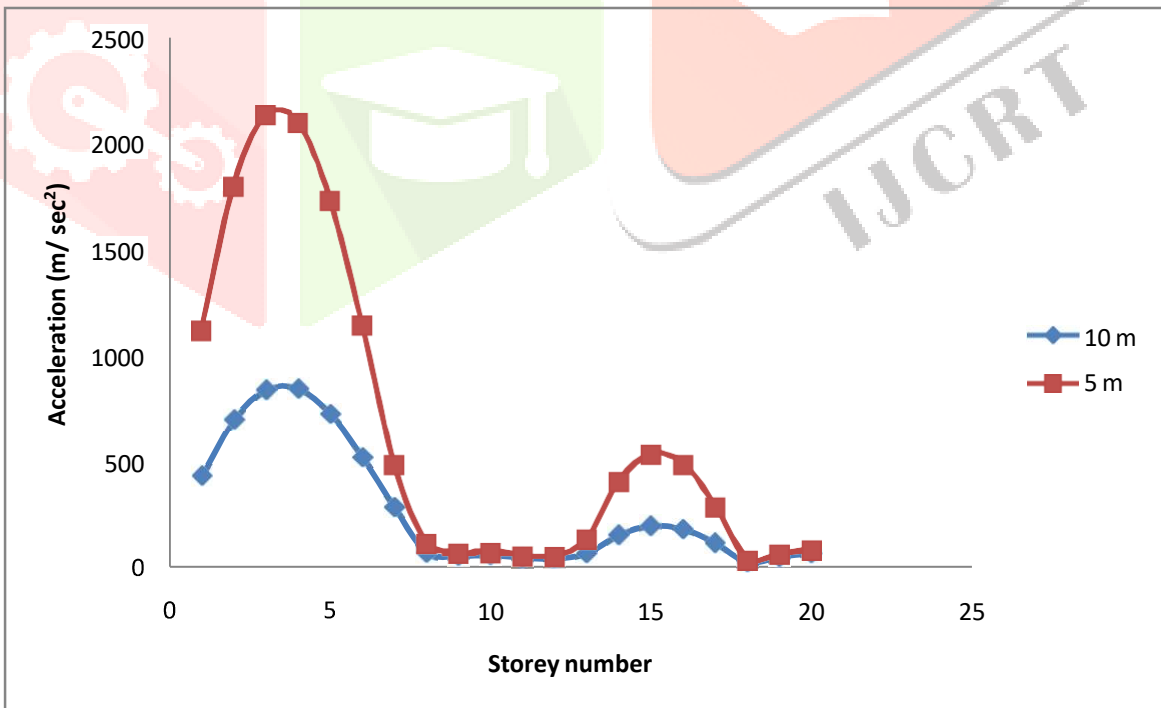


Figure 6.34: Acceleration vs. storey plot for 20 storey building

Figure 6.33 to figure 6.37 shows the plot of joint acceleration value of each floor for 25, 20, 15, 10 and 5 storey RC building. Two cases were also selected to analyze acceleration behavior of the structure by varying stand-off distance. The stand-off distance taken was 5m and 10m. The results were plotted and analyzed.

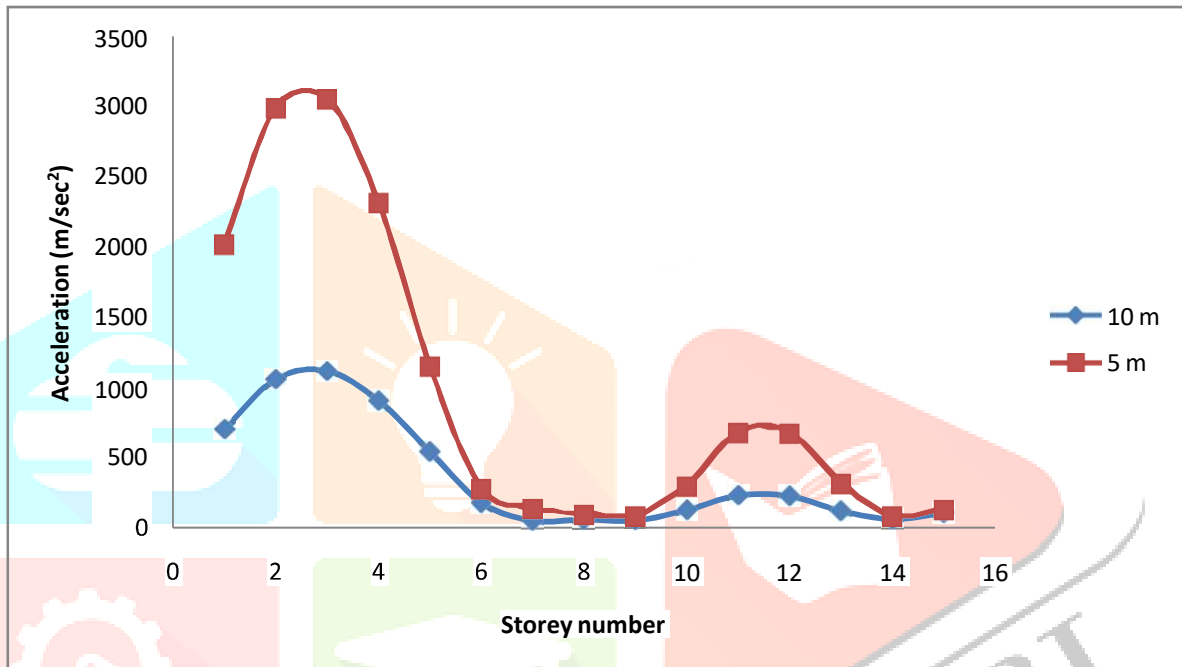


Figure 6.35: Acceleration vs. storey plot for 15 storey building

The joint acceleration value increases with decrease in height of structure. From all the figures, similar trend were observed except the structure having 5 storeys, where peak occurred at 1st storey. The difference in peak value increases as the structure height reduces. The maximum joint acceleration value for five storey building was 8000 m/sec² and 2000 m/sec² when the stand-off distance was 5 m and 10 m respectively. Therefore stand-off distance plays a major role in structural behavior subjected to blast load. By reducing stand-off distance to half, very high difference in joint acceleration value is observed.

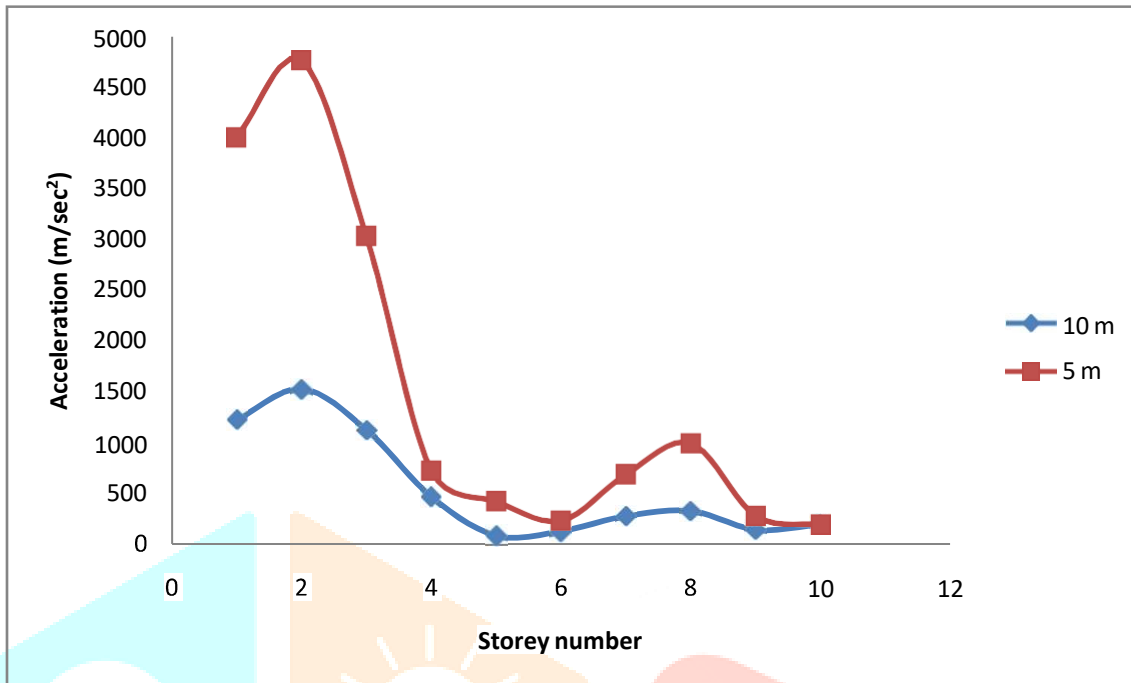


Figure 6.36: Acceleration vs. storey plot for 10 storey buildings

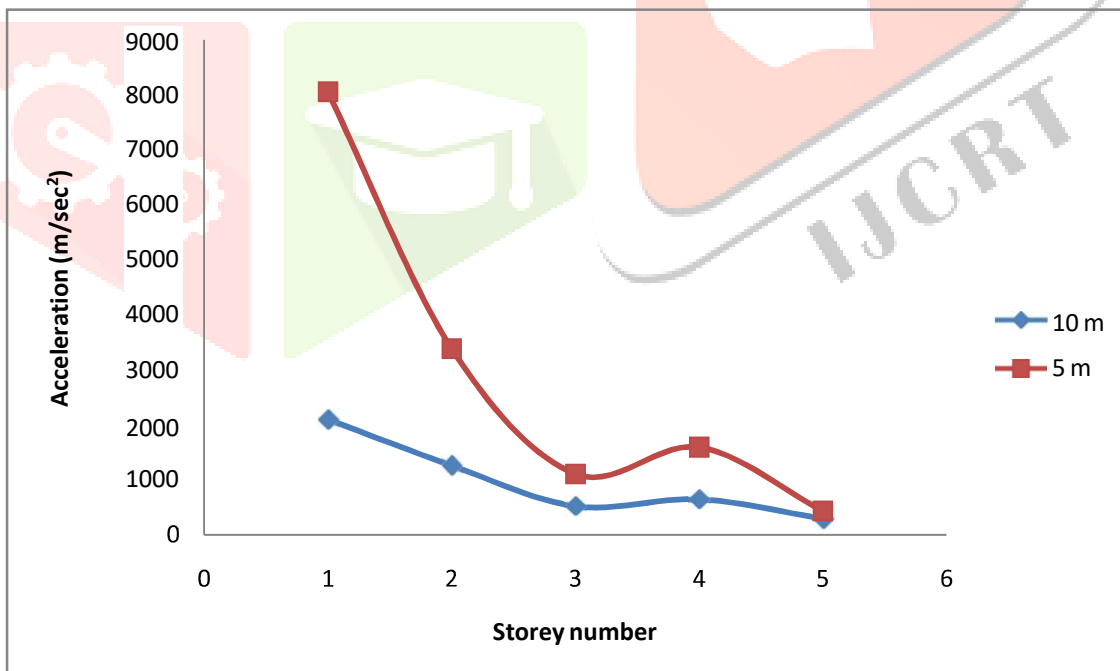


Figure 6.37: Acceleration vs. storey plot for 5 storey buildings

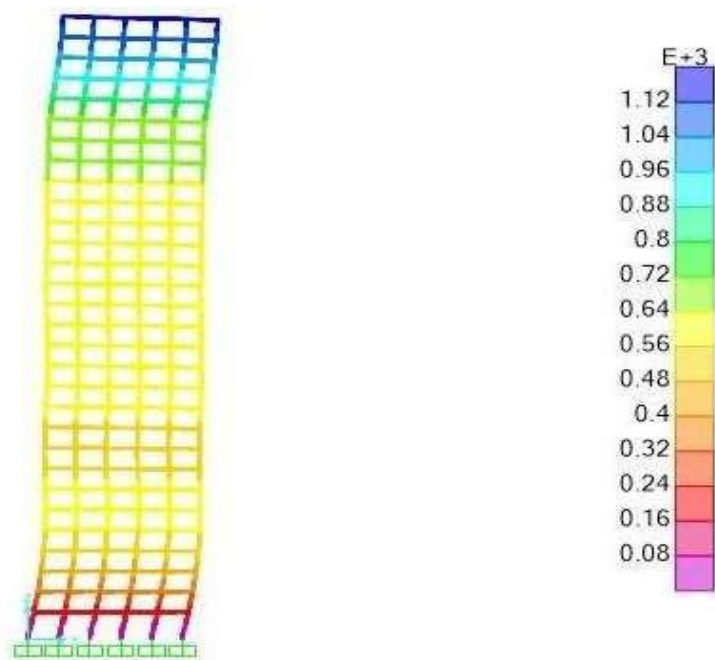


Figure 6.38: Deflection contour of 30 storey building. (unit in mm)

Figure 6.38 shows the deflection diagram of a 30 storey structure subjected to blast load. Contours are used to show the deflection by various colors

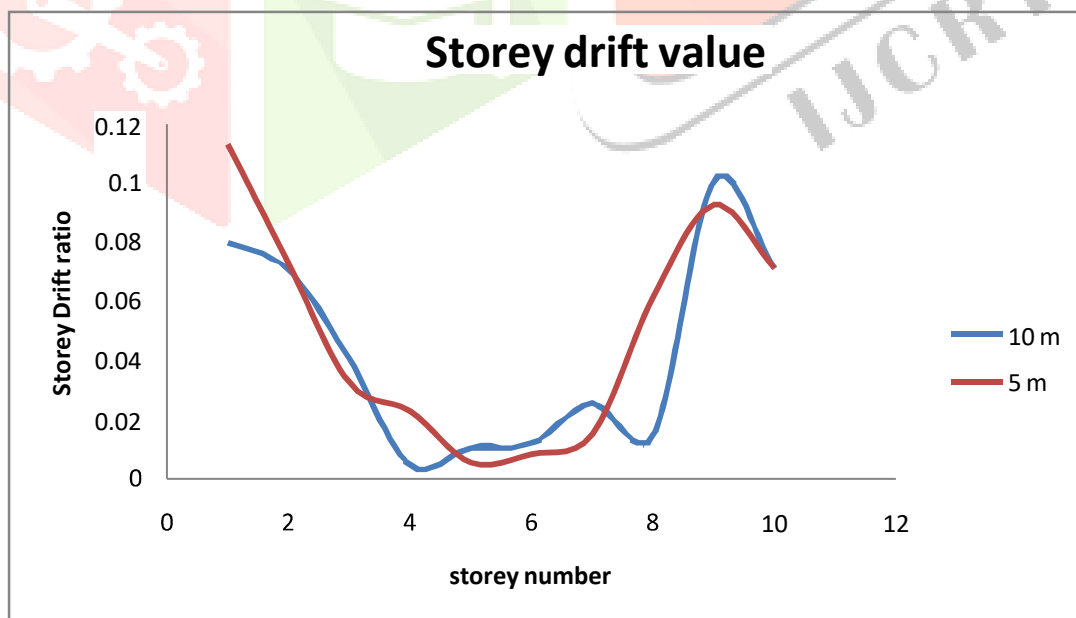


Figure 6.39: Storey drift ratio of 10 storey structure.

Figure 6.39 shows the storey drift ratio value of a 10 storey building. The definition of storey drift is “It is the displacement of one level relative to the other level above or below” [IS 1893 (part 1):2002]. The results were plotted by varying stand-off distance. The stand-off distance was 5 m and 10 m. For the first floor, the value was maximum. Its value reduces till 4th floor. Then it nearly becomes constant. After 7th floor it starts increasing. On the 9th floor it reaches peak. For the 10th floor there is a small dip in the value. For both cases, the results were similar. On 4th floor the value was more for 5 m stand-off distance. On the 9th floor, 10 m stand-off distance shows more value.

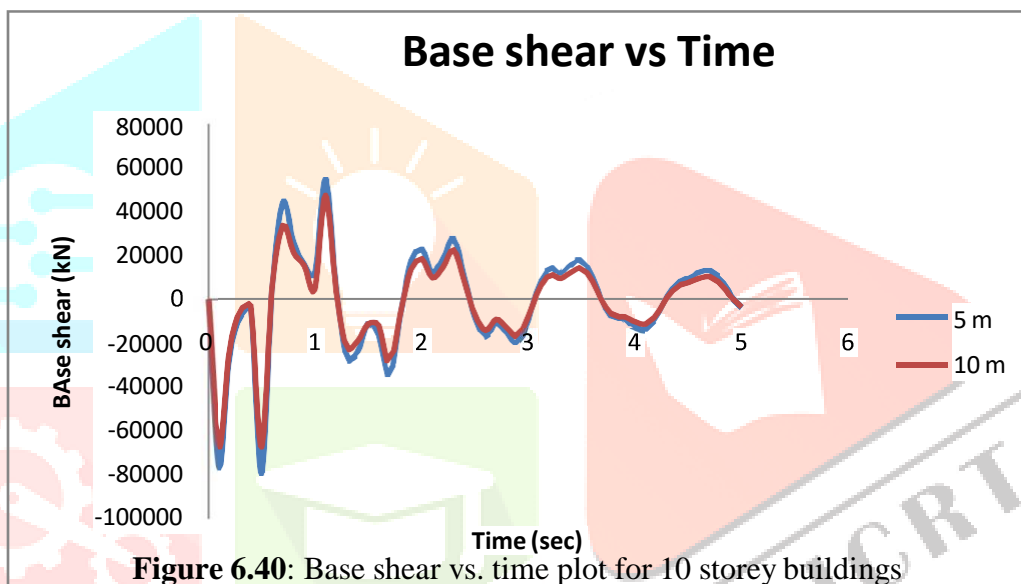


Figure 6.40 shows the variation of base shear with time for a 10 storey building by varying stand-off distance. The output time step size was 0.1 sec. Total steps taken were 50. Similar trends were followed for both the cases. The base shear value is mainly concentrated till 2 seconds. The peak observed was 80000 kN and 68000 kN for stand-off distance of 5m and 10 m respectively. After 5 seconds, the value is diminished to zero.

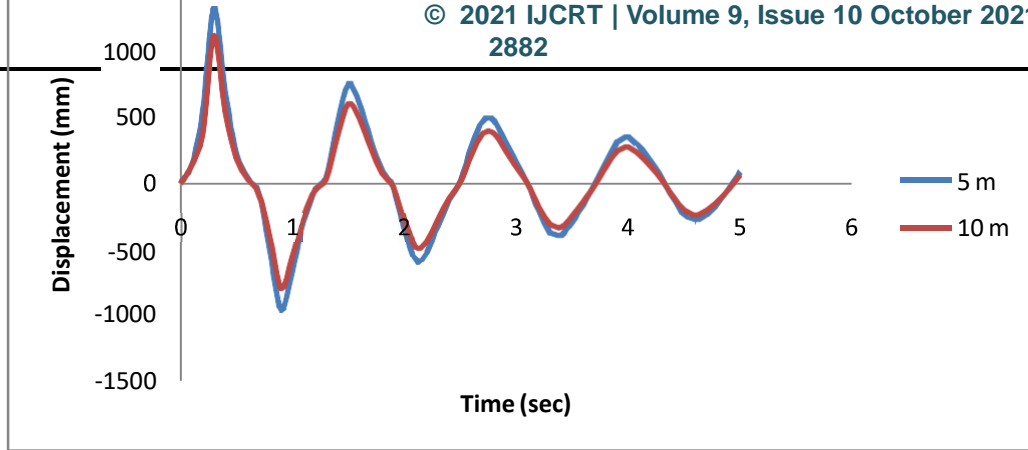


Figure 6.41: Displacement vs. time plot for 10 storey buildings

Figure 6.41 shows the plot of displacement of top floor joint of a 10 storey building subjected to blast load. The maximum deflection occurs just after the blast strikes the structure. The curve follows sinusoidal pattern but with less peak as the time progresses. After 6 sec the vibration stops and the structure becomes stationary.

From the above observations, we can conclude that stand-off distance is the most important parameter. The blast wave follows exponential pattern with distance and time. So by changing stand-off distance to half, there is considerable increase on blast load values. If the stand-off distance is more, the damage on the structure will be less. Therefore to achieve this we may provide a rigid fencing to avoid near field explosion. This will increase the stand-off distance.

6.4 Comparison between CSA Standard S850-12 (2012) and IS: 4991 (1968)

Table 6.2 shows joint load and duration of load application for 10 storey RC building. The load and time are calculated by both Indian codes [IS: 4991 (1968)] and Canadian codes [CSA Standard S850-12 (2012)] respectively. The load shown is for middle joints of each floor. From the table, it is evident that joint load on first floor is more for the case of Canadian code. For other floors, joint load is more for the case of Indian code. Time duration is more for the case of Canadian code for each floor. On the tenth floor the load is nearly same.

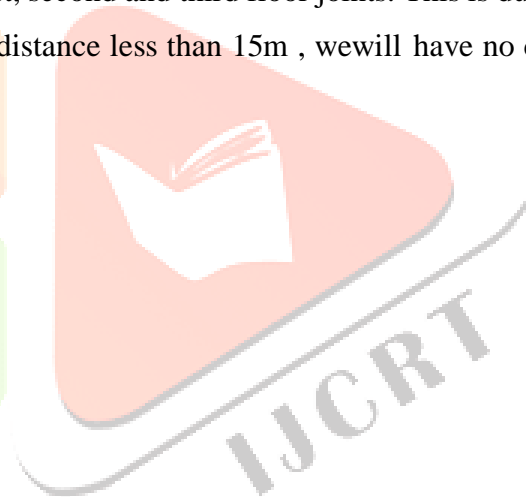
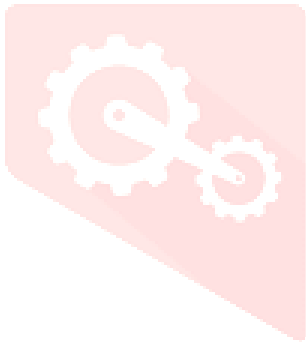
Table 6.2: Load and time calculation files for 10 storey building

Joint	IS: 4991 (1968)		CSA Standard S850-12 (2012)	
	Load (kN)	Time (ms)	Load (kN)	Time (ms)
1				
2				
3				
4				
5				
6				
7				
8				
9				
10				

R1	97943.04	5.39	115640.03	20.3514
R2	65295.36	5.39	53109.17	22.0798
R3	60115.68	5.39	35571.08	21.8141
R4	45126	6.3	22965.4	20.8049
R5	28998.36	7.9	15113.6	20.2539
R6	19415.95	9.7	10326.79	20.9977
R7	12980.59	11.4	7192.014	22.6544
R8	8789.76	13.3	5267.924	25.01
R9	7298.64	15.4	4022.458	27.9294
R10	3413.88	16.2	3178.08	30.8889

Time duration calculated by Indian code is same for first, second and third floor joints. This is due to fact that minimum scale distance is 15 m. Therefore for scaled distance less than 15m , we will have no choice other than to take same value of 5.39 milliseconds.

$$\text{Scaled distance} = \frac{R}{W^3} \quad (6.1)$$



Here W is in ton for and kg for Indian codes [IS: 4991 (1968)] and Canadian codes [CSAStandard S850-12 (2012)] respectively. W is the weight of explosive.

Figure 6.42, 6.43 and 6.44 shows the plot between storey and displacement, velocity and acceleration respectively for both the cases.

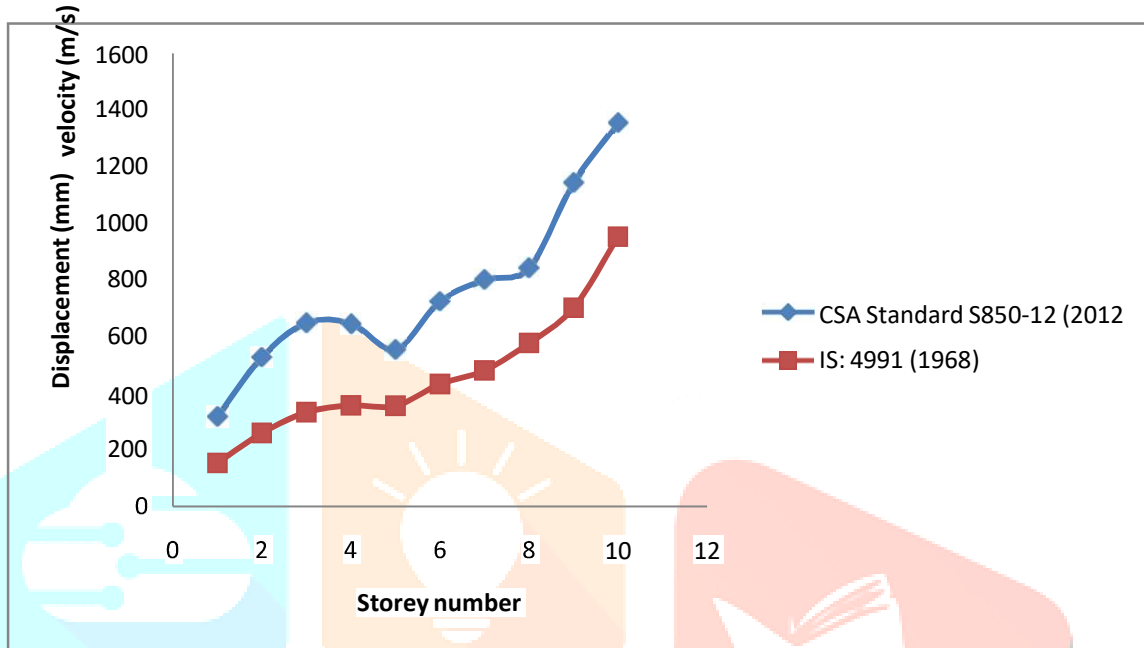


Figure 6.42: Displacement vs. storey plot for 10 storey building

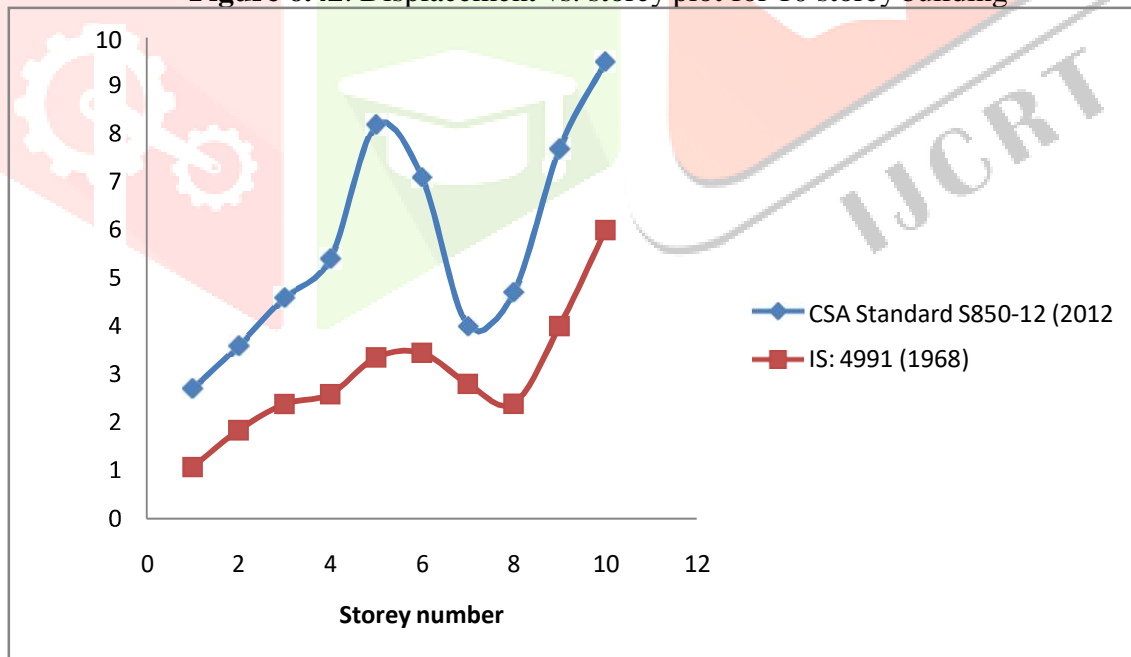


Figure 6.43: Velocity vs. storey plot for 10 storey building

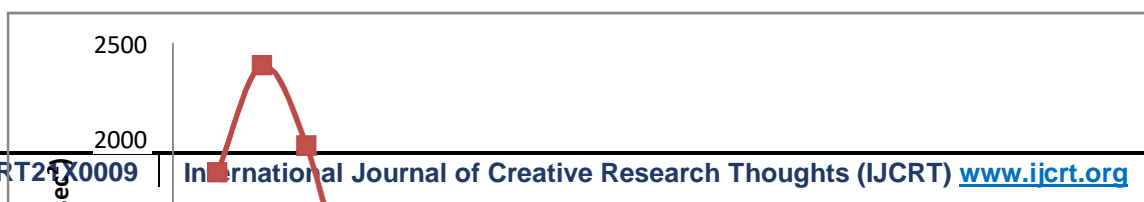


Figure 6.44: Acceleration vs. storey plot for 10 storey building

From table 6.2, the output displacement, velocity and acceleration obtained is more for the case of application of loads by Canadian code for each floors. For both the cases the displacement is maximum for tenth floor, velocity is maximum for fifth floor and acceleration is maximum for second floor. From the plots it is clear that there is huge difference in the result obtained by both the codes. Canadian code is newer and Indian code is older. Also there are various and separate formulas for load and calculation for different ranges of scaled distance. On the other hand there is no specific formula given for load calculation in Indian code. Some standard values are given. For intermediate value we have to interpolate between two values. Also it gives conservative results. So we may assume that results obtained by Canadian code are much more real than Indian code. Also the value starts from 15 m scaled distance. So the Indian code is not suitable for near field explosions. The code should be modified so that it includes all aspects of blast loading as per the current scenario.

CHAPTER - 7

CONCLUSIONS

Chapter 7

CONCLUSIONS

7.1 Conclusions

This paper presents result for various 3-d framed concrete structures subjected to blast loading using SAP 2000. The objective of the analysis is to understand the response of structure. The following conclusions can be drawn from this research as follows:

- The use of user-defined plastic hinges provides realistic behavior of structures subjected to blast loading.
- When the detonation point is along the center line of buildings, the interior columns take the majority of blast loads, not the side and the corner columns. Therefore for this scenario, the stiffness and strength of interior columns should be increased by increasing the size of it.
- Stand-off distance plays a major role in blast loading environment. By increasing the stand-off distances, the effect of surface explosions can be minimized. So, by providing a rigid concrete fence or wall around the structure would help in avoiding the explosion near the structure.
- For a 10 storey building, reducing stand-off distance by 5m causes enormous increase in base shear value. The base shear values for stand-off distances 5m and 10 m were 80000 kN and 68000 kN respectively.
- The peak storey drift ratio value observed for 10 m stand-off distance and 5 m stand-off distance was 0.08 and 0.116 respectively. It occurred on 1st storey of the structure. On the 9th storey, there is significant storey drift ratio value.
- Low-rise structures are more vulnerable to blasting as compared to high-rise building as blast loads are mainly applied on bottom 2 or 3 floors. This happens because blast wave decreases exponentially when stand-off distance increases.
- Indian code is very old drafted in 1968. There is no specific formula given for blast load calculation in Indian code and the scaled distance value starts from $15 \text{ m/t}^{1/3}$. So the Indian code is not suitable for near field explosions. The code should be modified so that it includes all aspects of blast loading as per the current scenario.

For high risk structures, design considerations against extreme load are important. Blast resistant design refers to maintaining the integrity of structure instead of its total collapse or partial collapse. Therefore, proper guidelines or stipulations for abnormal or extreme load cases should be included in current building regulation codes and structural design standards.

References

- T, Ngo., P, Mendis., A, Gupta. and J, Ramsay (2007) "Blast loading and Blast effects on structure-an overview." *EJSE Special Issue: Loading on Structures*.
- Chiranjeevi, M.D. and Simon, J. (2016) "Analysis of Reinforced Concrete 3d Frame under Blast Loading and

Check for Progressive Collapse.” *Indian Journal of Science and Technology*

- IS: 4991 (1968) “Criteria for blast resistant design of structures for explosions above ground.” *Bureau of Indian Standards*, New Delhi, India.
- IS: 875 Part 1 (1987) “Code of practice for design loads (other than earthquake) for buildings and structures.” *Bureau of Indian Standards*, New Delhi, India.
- IS: 875 Part 2 (1987) “Code of practice for design loads (other than earthquake) for buildings and structures.” *Bureau of Indian Standards*, New Delhi, India.
- Karlos, V., and Solomos, G. (2013) “Calculations of blast loads for application to structural components.” *JRC technical reports, European commissions*.
- Unified Facilities Criteria (2008) “UFC 3-340-02 Structures to Resist the Effects of Accidental Explosions”, *U.S. Army Corps of Engineers, Naval Facilities Engineering Command, Air Force Civil Engineer Support Agency*.
- T. Ngo, P. Mendis, A. Gupta & J. Ramsay, “ Blast Loading and Blast Effects on structure”, *The University of Melbourne*, Australia, 2007.
- F. Fu. “Dynamic response and robustness of tall buildings under blast loading”, *J. Constr. Steel Res.* 80(2013), 299-307
- H.M Elsananadedy, T.H. Almuallam, Y.R. Alharbi, Y.A. Al-Salloum, H. Abbas, progressive collapse potential of a typical steel building due to blast attacks, *J. Constr. Steel Res.* 101(2014) 143-157
- Malvar, L.J. (1998) “Review of static and dynamic properties of steel reinforcing bars. *ACI Materials Journal*”, 95(5), 609–616.
- Soroushian, P., and Choi, K. (1987) “Steel mechanical properties at different strain rates”. *Journal of Structural Engineering.*, 113(4), 663–672.
- CEB (Comite Euro-International du Beton). (1993) “*CEB-FIP Model Code 1990* ”., Redwood Books, Trowbridge, UK.
- Grote, D.L., Park, S.W., and Zhou, M. (2001) “Dynamic behaviour of concrete at high strain rates and pressures: I experimental characterization”. *International Journal of Impact Engineering.*, 25(9), 869–886.
- Tedesco, J.W., Powell, J.C., Ross, C.A., and Hughes, M.L. (1997) “A strain-rate dependent concrete material model for ADINA”. *Computer and Structure.*, 64(5/6), 1053–1067.
- Tedesco, J.W., and Ross, C.A. (1998) “Strain-rate-dependent constitutive equations for concrete”. *ASME Journal of Pressure Vessel Technology.*, 120(4), 398–405.
- Alexander, M. (2003) “A review of methods for predicting bomb blast effect on buildings”, *Journal of battlefield technology.*, 6(3), 155-161.
- Khatavakar, n., Prasad, B.K.R., and Amarnath, K. (2016) “Response of high rise structures subjected to blast loads.” *International journal of Science Engineering and Technology Research.*, 5(7).
- Goel, M.D., Agrawal, D., and Choubey, A. (2017) “Collapse behavior of RCC Building under blast load.” *Procedia Engineering.*, 173(2017), 1943-1950

- Silva,P.F., and Lu B.(2009) “Blast Resistance Capacity of Reinforced Concrete Slabs. ”*Journal of Structural Engineering.*,135, 708
- Ronald L. Shope (2006), “Response of wide flange steel columns subjected to constant axial load and lateral blast load”. *Civil Engineering Department, Blacksburg, Virginia*
- Soroushian, P., and Choi, K. (1987) “Steel mechanical properties at different strain rates”. *Journal of Structural Engineering.*,113 (4),663–672.
- Saatcioglu,M., Lloyd,A., and Jacques, E. (2011)“Focused Research for the Development of a CSA Standard on Design and Assessment of Buildings Subjected to Blast Loads.” *Hazard Mitigation and Disaster Management Research Centre Publication.* Univ. of Ottawa, Ottawa.
- Khan,S.,Saha,S. K., Matsagar,V.A., and Hoffmeister,B.“Fragility of Steel Frame Buildings under Blast Load.” *Journal of Performance of Constructed Facilities.* ASCE, ISSN 0887-3828.
- Meghanadh,M., and Reshma,T.(2017) “BLAST ANALYSIS AND BLAST RESISTANT DESIGN OF R.C.C RESIDENTIAL BUILDING.”*International Journal of Civil Engineering and Technology (IJCIET).*,8(3),761–770.
- Shallah,O., Eraky,A., Sakr,T., and Emad,S.(2014) “Response of Building Structures to Blast Effects.”*International Journal of Engineering and Innovative Technology (IJEIT).*,4(2).
- Goel,M.D.,Matsagar,V.A.,Gupta,A.K.,and Marburg,S.(2012)“An Abridged Review of Blast Wave Parameters.”*Defence Science Journal.*,62(5),,300-306
- Hashemi,A., and Mosalam,K.M.(2004) “Transient analysis of reinforced concrete frame with and without masonry infill wall under blast.”*Emirates Journal for Engineering Research.*,9(2), 97-103
- Ibrahim,Y.E.,Ismail,M.A and Nabil,M.(2017)“Response of reinforced concrete frame structures under blast loading.” *Procedia Engineering.*,171,890-898
- Williams, G., Batho, S., and Russell L.(2000) “ Responding to Urban Crisis.” *The emergency planning response to the bombing of Manchester city centre Cities.*,17, 293 – 304
- Manning,W.A.(1993)“The World Trade Center bombing: report and analysis.” *US fire administration / technical report series, USFA-TR-076*
- Oстераas, J.D.,(2006), “Murrah Building Bombing Revisited: A Qualitative Assessment of Blast Damage and Collapse Pattern.” *Journal of Performance of Constructed Facilities.*,20,330
- Rasbash, D.J., Ramachandran, G., Kandola, B., Watts, J.M., and Law, M.(2004) “Evaluation of fire safety.” *Johan Wiley and Sons Ltd.* ISBN 0-471-49382-1
- Bao,X., and Li, B.(2010) “Residual Strength of Blast Damaged Reinforced Concrete Columns.” *International Journal of Impact Engineering.*, 37(3), 295-308
- Liew, J. 2008) “Survivability of Steel Frame Structures Subject to Blast and Fire.” *Journal of Constructional Steel Research.*,64,854-866
- Biggs, J.M.(1964) “Introduction to Structural Dynamics.”*McGraw-Hill, New York*

- Baker, W.E., Cox, P.A., Westine, P.S., Kulesz, J.J., and Strehlow, R.A. (1983) “*Explosion Hazards and Evaluation.*” Elsevier, New York
- Yandzio, E., and Gough, M. (1999) “Protection of Buildings against Explosions.” *Steel Construction Institute.*
- BBC News. (2013) “Reims blast and building collapse in France kills three.”
<http://www.bbc.co.uk/news/world-europe-22328568>
- CBS News. (2013) “11 still unaccounted for after Argentina building explosion.” http://www.cbsnews.com/8301-202_162-57597667/11-still-unaccounted-for-after-argentina-building-explosion.
- Johansson, M. (2002) “Shockwave propagation in air.” *Swedish Rescue Services, Karlstad, Sweden.*
- Craighead, G. (2009) “High-rise security and fire life safety.” *Butterworth-Heinemann, ISBN: 978-1856175555*
- Hashemi, A., and Mosalam, K.M. (2004) “Transient analysis of reinforced concrete frame with and without masonry infill wall under blast.” *Emirates Journal for Engineering Research*, 9(2), 97-103.
- ASCE/SEI 59-11 (2011). “Blast Protection of Buildings.”
- CSA Standard S850-12 (2012) “Design and assessment of buildings subjected to blast loads.” *Canadian Standard Association, ON*
- Asaeda, G. (2007) “*World Trade Center Attack, NYFD.*”
www.yalenewhavenhealthorg/emergency/2005CONGRESS/Day1Track3/Asaeda.pdf
- Draganić, H., and Sigmund, V. (2012) “Blast loading on structures.” *Technical Gazette*, 19(3), 643-652.
- Patil, V.B., Bhilare, L.S., and Patil, G.R. (2016) “Effect of Blast Load on Soft Storey Building.” *International Journal on Recent and Innovation Trends in Computing and Communication*, 4(10), 13-20.
- IS: 1893 part 1 (2002) “Criteria for Earthquake resistant design of structures.” *Bureau of Indian Standards, New Delhi, India.*